Molecular Pharmacology Fast Forward. Published on January 13, 2006 as doi:10.1124/mol.105.019299


MOL # 19299

# Discovery of naturally occurring splice variants of the rat histamine $H_3$ receptor that act as dominant negatives*

Remko A. Bakker, Adrian Flores Lozada, André van Marle, Fiona C. Shenton, Guillaume Drutel, Kaj Karlstedt, Marcel Hoffmann, Minnamaija Lintunen, Yumiko Yamamoto, Richard M. van Rijn, Paul L. Chazot, Pertti Panula, and Rob Leurs.

The Leiden/Amsterdam Center for Drug Research, Department of Medicinal Chemistry, Vrije Universiteit Amsterdam, De Boelelaan 1083, 1081HV Amsterdam, The Netherlands (*RAB*, *AvM*, *GD*, *MH*, *RMvR*, *RL*)§.

The Department of Biology, Åbo Akademi University, Biocity, Artillerigatan 6A, FIN-20520 Turku, Finland (*AFL*, *KK*, *ML*, *YY*, *PP*).

The Neuroscience Center, and Institute of Biomedicine/Anatomy, University of Helsinki, POB 63, FIN-00014 Helsinki, Finland (*PP*).

The School of Biological and Biomedical Sciences, University of Durham, South Road, DH1 3LE Durham, UK (*FCS*, *PLC*).

Molecular Pharmacology Fast Forward. Published on January 13, 2006 as DOI: 10.1124/mol.105.019299
This article has not been copyedited and formatted. The final version may differ from this version.



RUNNING TITLE PAGE

a) Running title: Discovery of dominant negative rat histamine $H_3$ isoforms.

b) Address correspondence to:

Prof. Dr. R. Leurs

The Leiden/Amsterdam Center for Drug Research, Department of Medicinal Chemistry, Vrije Universiteit Amsterdam, De Boelelaan 1083, 1081HV Amsterdam, The Netherlands. Tel. ++31 20 5987579; Fax. ++31 20 5987610; E-mail: r.leurs@few.vu.nl

c) Number of:

| | |
|---|---|
| Text pages: | 42 |
| Tables: | 0 |
| Figures: | 8 |
| References: | 47 |
| Words in the *Abstract*: | 235 |
| Words in the *Introduction*: | 561 |
| Words in the *Discussion*: | 1720 |

d) List of Non-standard abbeviations: GPCR, G-protein coupled receptor; seven-transmebrane-domain, 7TM; 7TM-r$H_3$R isoforms, the r$H_{3A}$, r$H_{3B}$, and r$H_{3C}$ receptors; 6TM-r$H_3$R isoforms, the the r$H_{3D}$, r$H_{3E}$, and r$H_{3F}$ isoforms; Pertussis Toxin, PTX; PTZ, pentylenetetrazole; $^{125}$I-APT, [$^{125}$I]aminopotentidine; $^{125}$IPP, [$^{125}$I]iodophenpropit; ELISA, Enzyme-linked Immunosorbent Assay.

Molecular Pharmacology Fast Forward. Published on January 13, 2006 as DOI: 10.1124/mol.105.019299
This article has not been copyedited and formatted. The final version may differ from this version.



## ABSTRACT

We previously described the cDNA cloning of three functional rat histamine $H_3$ receptor ($rH_3R$) isoforms as well as the differential brain expression patterns of their corresponding mRNAs and signalling properties of the resulting $rH_{3A}$, $rH_{3B}$, and $rH_{3C}$ receptor isoforms (Drutel *et al*. (2001) *Mol Pharmacol*. 59:1-8). Herein we describe the cDNA cloning, mRNA localisation in the rat CNS and a pharmacological characterisation of three additional $rH_3R$ splice variants ($rH_{3D-F}$) that differ from the previously published isoforms in that they result from an additional alternative-splicing event. These new $H_3R$ isoforms lack the seventh transmembrane (TM) helix and contain an alternative, putatively extracellular, C-terminus (6TM-$rH_3$ isoforms). After heterologous expression in COS-7 cells, radioligand binding or functional responses upon the application of various $H_3R$ ligands could not be detected for the 6TM-$rH_3$ isoforms. In contrast to the $rH_{3A}$ receptor ($rH_{3A}R$), detection of the $rH_{3D}$ isoform using HA-antibodies revealed that the $rH_{3D}$ isoform remains mainly intracellular. The expression of the $rH_{3D-F}$ splice variants, however, modulates the cell surface expression-levels and subsequent functional responses of the 7TM $H_3R$ isoforms. Co-expression of the $rH_{3A}R$ and the $rH_{3D}$ isoforms resulted in the intracellular retention of the $rH_{3A}R$ and reduced $rH_{3A}R$ functionality. Finally, we show that in rat brain the $H_3R$ mRNA expression levels are modulated upon treatment with the convulsant pentylenetetrazole, suggesting that the herein described $rH_3R$ isoforms thus represent a novel physiological mechanism for controlling the activity of the histaminergic system.

Molecular Pharmacology Fast Forward. Published on January 13, 2006 as DOI: 10.1124/mol.105.019299
This article has not been copyedited and formatted. The final version may differ from this version.



## INTRODUCTION

Histamine receptors are members of the superfamily of seven-transmebrane-domain (7TM) G-protein coupled receptors (GPCRs). The $H_3R$ was pharmacologically identified in 1983 and holds great promise as a target for the development of therapeutics for numerous disorders, including obesity, epilepsy and cognitive diseases such as attention deficit hyperactivity disorder (ADHD) and Alzheimer's disease (see Bakker, 2004; Leurs et al., 2005 for reviews). The cloning of the histamine $H_3$ receptor ($H_3R$) cDNA allowed for the subsequent cloning of related sequences, including a variety of $H_3R$ isoforms from different species (see Bakker, 2004; Leurs et al., 2005 for reviews).

Alternative splicing of pre-mRNA represents a widespread mechanism for increasing the variability of eukariotic gene expression by generating structurally distinct isoforms from a single gene. Alterations in the expression of GPCR isoforms could be associated with disease (Schmauss et al., 1993). Although $\alpha_1$-AR adrenoceptors and dopamine receptors are prime examples of alternatively spliced GPCRs (Cogé et al., 1999; Hawrylyshyn et al., 2004; Kilpatrick et al., 1999), more and more GPCR splice variants are identified for other members of the GPCR superfamily. A variety of $H_3R$ isoforms from several species have been reported (see Bakker, 2004; Leurs et al., 2005 for reviews). In addition to the 445 amino acids containing $rH_{3A}R$ two presumably non-functional truncated isoforms (reported as $rH_{3T}$ or $rH_{3(nf1)}$ and $rH_{3(nf2)}$) (Drutel et al., 2001; Morisset et al., 2001), and three functional $rH_3R$ isoforms have been detected: $rH_{3B}$, $rH_{3C}$, and the $rH_{3(410)}$ receptor, generated by deletions in the third intracellular loop of the $rH_3R$ of 32, 48, and 35 amino acids, respectively. Since several $H_3R$ isoforms have been shown to possess specific pharmacological characteristics in terms of ligand-binding and

Molecular Pharmacology Fast Forward. Published on January 13, 2006 as DOI: 10.1124/mol.105.019299
This article has not been copyedited and formatted. The final version may differ from this version.



initiation of signal-transductions events (Drutel et al., 2001), the $H_3R$ mRNA splicing can significantly affect cellular responses to histamine. A detailed understanding of the spectrum of $H_3R$ splice variants in different species is of importance not only for the understanding of histaminergic system, but also for future drug development efforts.

In the present study we describe the identification of three additional 6TM-r$H_3$ isoforms following an RT-PCR approach using rat brain cDNA. While the mRNA for these 6TM-r$H_3$ isoforms is detected in the rat brain, in attempting their characterisation, we failed to detect radioligand binding using $H_3R$ specific radioligands as well as functional effects upon heterologous expression in COS-7 cells. Co-expression of 7TM-r$H_3$Rs with the 6TM-r$H_3$ isoforms, however, revealed that the 6TM-r$H_3$ isoforms inhibit the cell surface trafficking and subsequent functional activity of the 7TM-r$H_3$Rs. The regulation of the expression of the 6TM-r$H_3$ isoforms may therefore represent a novel mechanism for the regulation of $H_3R$ functionality. To study possible *in vivo* functional relationships between 7TM-r$H_3$R and 6TM-r$H_3$ isoforms relative expression levels were analyzed in a model of generalized tonic-clonic seizures induced by pentylenetetrazole (PTZ). Data from a study on kainic acid-induced status epilepticus indicates that systemic kainic acid induces a direct or indirect selective increase in $H_3R$ isoforms with a full third intracellular loop in areas which suffer rapid neuronal damage (Lintunen et al., 2005). Currently, no data is available whether 7TM-r$H_3$R and 6TM-r$H_3$ isoforms are similarly regulated under pathophysiological conditions in the rat brain. The PTZ seizure model used in this study allows us to determine if an $H_3R$ isoform specific response occurs in a pathological setting. Our findings therefore uncover a new mechanism that may control the regulation of $H_3R$ activity in the brain.

Molecular Pharmacology Fast Forward. Published on January 13, 2006 as DOI: 10.1124/mol.105.019299
This article has not been copyedited and formatted. The final version may differ from this version.



## MATERIALS AND METHODS

*Materials*. Immepip, clobenpropit, and thioperamide were synthesised at the department of Medicinal Chemistry at the Vrije Univeristeit Amsterdam. Gifts of $pcDEF_3$ (Dr. J. Langer), pTLN21CRE-Luc (Dr. W. Born) and of the cDNAs encoding the PTX insensitive mutant rat $G\alpha_{i/o}$ proteins $G\alpha_{i1}C^{351}I$, $G\alpha_{i2}C^{352}I$, $G\alpha_{i3}C^{351}I$, and $G\alpha_oC^{351}I$ (Dr. G. Milligan, University of Glasgow, UK), the cDNA encoding the FLAG-tagged $rH_{3A}R$ (Dr. F. Cogé, Institut de Recherches Servier), the cDNA encoding the human histamine $H_1$ receptor (Dr. H. Fukui, University of Tokushima, Tokushima, Japan), the cDNA encoding the KSHV-GPCR ORF74 (Dr. T. Schwartz, University of Copenhagen), mianserin hydrochloride (Organon NV, The Netherlands), and the HA-antibody and Rhodamine labelled secondary antibody (Dr. J. van Minnen, Vrije Universiteit Amsterdam, The Netherlands), are greatly acknowledged. All other materials were from commercial suppliers.

*Constructs.* The reverse transcription and PCR amplification for cloning of the $rH_{3D-F}$ (6TM-$rH_3$) isoform cDNAs were performed as described (Drutel et al., 2001). The full-length cDNAs were isolated with primers overlapping the rat $H_3R$ cDNA sequence. The forward sequence included a Kozak sequence (underlined) (5'-CCG CCA CCA TGG AGC GCG CGC CGC CCG ACG GGC TG-3'). The reverse sequence was based on cDNA for rat orphan GPCR (Genbank accession number AB015646) (5'-CTC TAC CCC ATA ACC ACC CAC C-3'). The use of these primers resulted in the amplification of at least 3 different products. After cloning in pCRII-TOPO the cDNAs were sequenced on both DNA strands and subcloned in $pcDNA_3$. The sequence of the identified $rH_{3F}$ isoform is identical to one of the sequences found in the GenBank® database (accession number AB015646, GI: 6681587), the sequences of the $rH_{3D}$ and $rH_{3E}$ isoforms have

Molecular Pharmacology Fast Forward. Published on January 13, 2006 as DOI: 10.1124/mol.105.019299
This article has not been copyedited and formatted. The final version may differ from this version.



been deposited in the GenBank® database (accession number DQ112342 and DQ112343, respectively). The hydropathic profile of the $H_{3D-F}$ isoforms was analysed using the TMHMM Server at the Center for Biological Sequence Analysis, Technical University of Denmark, DTU (http://www.cbs.dtu.dk/services/TMHMM/).

*Construction of rH₃R-G$_\alpha$ protein fusion constructs.* Fusion proteins between the rat $H_3R$ and PTX insensitive mutant rat Gα-proteins of the $G_{i/o}$ class were created by PCR using Turbo Pfu to remove the translation initiation codon from the Gα-protein cDNA sequence and the stop codon from the $rH_{3A}R$ cDNA sequence.

*HA-tagging of the rH₃R isoforms.* N-terminal hemagglutinin (HA)-tagged expression constructs of the $rH_{3A}R$ and $rH_{3D}$ isoform were generated by PCR (5'-GCC ACC ATG GGC TAC CCA TAC GAC GTC CCA GAC TAC GCC GCG GAG CGC GCG CCG C-3') and cloned into pcDNA 3.1 (Invitrogen, Leek). Construct integrity was verified by sequence analysis.

*Animals*. The study was conducted in accordance with the European Convention (1986) guidelines and approved by the local committee for Animal Experiments and the Provincial State Office of Western Finland and the Animal Ethics Committee of Abo Akademi University. Male Sprague-Dawley rats (260-280 g) were given PTZ (50 mg/kg, i.p.). Animals were stunned with $CO_2$ and killed by decapitation 6h (PTZ, n = 3), 24h (PTZ, n = 3), and 48h (PTZ, n = 3; saline control, n = 3) post-injection.

*In-situ hybridization histochemistry.* Probes were labeled with deoxyadenosine 5´-triphosphate, [α-$^{33}$P] (New England Nuclear, Boston, USA) at their 3´ ends using terminal deoxynucleotide transferase (Promega, Madison, WI), and subsequent *in-situ* hybridization histochemistry was

Molecular Pharmacology Fast Forward. Published on January 13, 2006 as DOI: 10.1124/mol.105.019299
This article has not been copyedited and formatted. The final version may differ from this version.



performed essentially as described previously (Drutel et al., 2001). The following oligo-probe sequence was used for detecting $H_{3DEF}$ isoform mRNAs: 5′-AAG TTT CCC GAG GCG CTC GAC ACA GTA ATC GGG GAT GCA GCG GCC-3′.

*Image analysis and data interpretation.* Autoradiographic films were quantified by digitizing the film images using the MCID 5+ image analysis system (Imaging Research, St. Catherines, Ontario, Canada) and by measuring gray scale pixel values. The relative optic density was converted to integrated optic density (IOD) based on a curve derived from $^{14}C$ standards exposed to films. Gray scale values were determined by using a total of four sections for each animal.

*Cell culture and transfection.* COS-7 African green monkey kidney cells were maintained and transfected as previously described (Bakker et al., 2004a; Drutel et al., 2001). HEK 293 cells were cultures under similar conditions and transfected with cDNA encoding the $rH_{3A}R$ using the LipofectaminePlus method according to the manufacturer's protocols.

*Reporter-gene assay.* $H_3R$ isoform-mediated modulation of cAMP mediated gene transcription activity was measured using the luciferase reporter-gene plasmid pTLNC121-3 (2.5 μg/1·$10^6$ cells) containing 21 cAMP-responsive elements. Luminescence was assayed 48hr after incubation of transfected cells with ligands as described previously (Bakker et al., 2004b).

*[$^{35}$S]GTPγS binding assays.* Transfected COS-7 cells were resuspended in 4°C binding buffer (20mM HEPES, 3μM GDP, 10mM $MgCl_2$, 150mM NaOH, pH 7.4). For measurement of agonist-stimulated GTPγS binding, 6μg of the crude cell extract was incubated in binding buffer with

Molecular Pharmacology Fast Forward. Published on January 13, 2006 as DOI: 10.1124/mol.105.019299
This article has not been copyedited and formatted. The final version may differ from this version.



ligands for 15 min at 30°C after which 0.1–0.2 nM [$^{35}$S]GTPγS (Perkin Elmer Life Sciences, 1250 Ci/mmol) was added to make a final total volume of 100μL. Bound radioactivity was separated by filtration after 15 min through Whatman GF/C filters on a Brandel cell harvester using 4°C wash buffer (20mM HEPES, 5mM $MgCl_2$, pH 7.4). Radioactivity retained on the filters was measured by liquid scintillation counting.

*Receptor binding studies.* Radioligand binding studies for the $H_1R$, $H_2R$, and $H_3R$ using [$^3$H]mepyramine, [$^{125}$I]aminopotentidine ($^{125}$I-APT), and [$N^{\alpha}$-methyl-$^3$H]histamine, respectively, were performed as described previously (Bakker et al., 2004b). The $H_3R$ radioligand binding studies using [$^{125}$I]iodophenpropit ($^{125}$IPP) were carried out under the same experimental conditions as for [$N^{\alpha}$-methyl-$^3$H]histamine. CXCL8 was labeled with $^{125}$I using the Iodogen method (Pierce, Rockford, Ill.) and subsequently used in ORF74 radioligand binding studies as described previously (Smit et al., 2002).

*Detection of tagged $rH_3Rs$.* In the enzyme-linked immunosorbent assays (ELISA), a mouse anti-hemagglutinin (anti-HA) monoclonal primary antibody was used as primary antibody, and a goat anti-mouse–horseradish peroxidase conjugate as secondary antibody for the detection of tagged $rH_3Rs$ in transfected cells. The 3,3',5,5'-tetramethylbenzidine liquid substrate system for ELISA was used as substrate and the optical density was measured at 450 nm using a Victor$^2$ Wallac multilabel counter (PerkinElmer, Boston, USA). The same primary antibody was used for immunocytochemistry in conjunction with a secondary rhodamine labelled Goat-anti-mouse antibody. Permeabilization of cells was achieved by an optional incubation of the cells for 5 min with 0.5% NP-40 in TBS prior to antibody application. For imaging, coverslips were mounted in

Molecular Pharmacology Fast Forward. Published on January 13, 2006 as DOI: 10.1124/mol.105.019299
This article has not been copyedited and formatted. The final version may differ from this version.



90% glycerol containing 0.02 M Tris-HCl (pH 8.0), 0.002% $NaN_3$, and 2% DABCO [1,4-diazabicyclo-(2,2,2)-octane; Merck, Darmstadt, Germany].

*Time-resolved FRET.* The *time-resolved* fluorescence resonance energy transfer (*tr*-FRET) experiments were conducted essentially as described previously (Bakker et al., 2004a). Energy transfer was measured by exciting the $Eu^{3+}$ at 320 nm and monitoring the allophycocyanin emission for 1000 μs at 665 nm using a Novostar (BMG Labtechnologies) configured for time-resolved fluorescence after a 50 μs delay.

*Cross-linking and immunoblotting of $rH_{3A}$ receptors.* Cells were harvested by centrifugation and the resulting pellet was resuspended in 150μl cross-linking buffer (150mM NaCl, 100mM Na-HEPES, 5mM EDTA pH7.5, 5mM DTT) to give a final protein concentration of approx. 0.5 mg/ml. The samples were incubated at room temperature with continual mixing for 12 minutes with either 0.12 or 0.25mM of the cell permeable cross-linker BS3 (bis(sulfosuccinimidyl)suberate), after which the cross-linking mixture was removed by centrifugation and the resultant pellet was used for immunoblotting as previously described (Chazot et al., 2001). Immunoblots were probed either with anti-$H_{3C}$ 188-197Cys antibody (Shenton et al., 2005) at a 0.2 μg/ml, or with an anti-$H_3$ 329-358 antibody used at a final protein concentration of 1.5μg/ml (Chazot et al., 2001).

*Analytical methods.* All data shown are expressed as mean ± S.E.M. Data from radioligand binding assays and functional assays data were evaluated by a non-linear, least squares curve-fitting procedure using Graphpad Prism® (GraphPad Software, Inc., San Diego, CA).

Molecular Pharmacology Fast Forward. Published on January 13, 2006 as DOI: 10.1124/mol.105.019299
This article has not been copyedited and formatted. The final version may differ from this version.



# RESULTS

### *Cloning of cDNAs encoding additional rat $H_3R$ isoforms.*

The existence of additional $H_3R$ isoforms was investigated by RT-PCR analysis of rat whole-brain total RNA using specific primers 1 and 2 (see *Materials and Methods*), and revealed the existence of three previously uncharacterised full-length cDNAs with putative corresponding proteins of 497 ($rH_{3D}$), 465 ($rH_{3E}$), and 449 ($rH_{3F}$) amino acids. The amino acid sequence of the $rH_{3F}$ isoform corresponds to one of the sequences found in the GenBank® database (accession number AB015646, GI: 6681587). These three new $rH_3$ isoforms correspond in a large part to the sequences of rat histamine $H_3R$ isoforms A, B and C ($rH_{3A}R$, $rH_{3B}R$, and $rH_{3C}R$, respectively) and exhibit exactly the same differences in length for the third intracellular loop (IL3) (Figure 1A). This insertion in IL3 in the $rH_{3D}$, $rH_{3E}$, and $rH_{3F}$ isoforms appears to be created by a retention/deletion system already described for the third intracellular loop (Cogé et al., 2001; Drutel et al., 2001; Morisset et al., 2001). However, the $rH_{3D}$, $rH_{3E}$, and $rH_{3F}$ isoforms differ from the $rH_{3A}R$, $rH_{3B}R$, and $rH_{3C}R$ in their C-terminal region, in which the last C-terminal 53 amino acids, which corresponding to the seventh transmembrane-domain and carboxy-terminus of the $rH_{3A}R$, $rH_{3B}R$, and $rH_{3C}R$ proteins, are replaced by a sequence of 105 amino acids that do not share any homology with the last 53 C-terminal amino acids of the $rH_{3A}R$, $rH_{3B}R$, and $rH_{3C}R$. Sequence analysis of the $rH_3R$ gene indicates that the alternative C-terminal domain that is found in the $rH_{3D-F}$ isoforms is due to a change in the open reading frame upon alternative splicing using previously unidentified exon/intron junctions present within the $rH_3R$ gene (see Figure 1B). Analysis of the hydropathic profile of the $rH_{3D}$, $rH_{3E}$, and $rH_{3F}$ isoforms does not reveal a clear putative seven transmembrane domain (Figures 2A and 2B).

Molecular Pharmacology Fast Forward. Published on January 13, 2006 as DOI: 10.1124/mol.105.019299
This article has not been copyedited and formatted. The final version may differ from this version.



Consequently, the $rH_{3D}$, $rH_{3E}$, and $rH_{3F}$ isoforms are predicted to possess only six transmembrane domains 6TM-$rH_3$ isoforms) and an extracellular C-teriminal domain (Figures 2C and 2D).

***Heterologous expression of epitope-tagged $rH_3R$ isoforms.***

Previously we have successfully characterised the $rH_{3A}R$, $rH_{3B}R$, and $rH_{3C}R$ using COS-7 cells heterologously expressing these receptors (Drutel et al., 2001). We therefore used the same approach in this study to characterise the herein described three additional 6TM-$rH_3$ isoforms. To evaluate the cell surface expression of the 6TM-$rH_3$ isoforms, we generated the cDNAs coding for the N-terminally HA-tagged $rH_{3A}R$ (HA-$rH_{3A}R$) and the N-terminally HA-tagged $rH_{3D}$ (HA-$rH_{3D}$) isoform by PCR. Whereas we detect clear immunological evidence for the cell surface expression of the HA-$rH_{3A}R$ using an ELISA assay utilizing anti HA-antibodies on intact cells, we can hardly detect the HA-$rH_{3D}$ isoforms on the cell surface on intact cells (Figure 2E). We observe, however, a clear immunofluorescent signal upon permeabilisation of cells expressing the HA-$rH_{3D}$ isoform (Figure 2E), indicating successful synthesis of the HA-tagged $rH_{3D}$ isoform protein and retention of the HA-tagged $rH_{3D}$ isoform inside the cell. There is an apparent difference in detection of the HA-$rH_{3D}$ isoform versus the HA-$rH_{3A}R$, which might indicate differences in e.g. the rate of synthesis, the inherent stability, or the rate of degradation of the $H_3$ isoforms, we have not pursued this issue further. To evaluate the plasma membrane localisation of the HA-$rH_{3A}R$ and the HA-$rH_{3D}$ isoform we subsequently performed immunocytochemistry studies using rhodamine labelled anti-HA antibodies. Plasma membrane localisation of the rhodamine-derived fluorescence was easily detected using cells expressing HA-$rH_{3A}Rs$ in intact cells (Figure 2F, *upper left* panel) and only a limited intracellular fluorescence was observed in NP40 permeabilised cells (Figure 2F, *upper right* panel). In contrast, corroborating the findings

Molecular Pharmacology Fast Forward. Published on January 13, 2006 as DOI: 10.1124/mol.105.019299
This article has not been copyedited and formatted. The final version may differ from this version.



obtained by the ELISA studies, using cells transfected with cDNA encoding the HA-r$H_{3D}$ isoform, appreciable rhodamine-derived fluorescence is only detected in permeabilised cells (Figure 2F, *bottom right* panel) and not on intact cells (Figure 2F, *bottom left* panel). Moreover, no plasma membrane localisation of the rhodamine-derived fluorescence was detected using permeabilised HA-r$H_{3D}$ isoform expressing cells. These data indicate an intracellular localisation for the HA-r$H_{3D}$ isoform.

***Are the 6TM-r$H_3$ isoforms functional $H_3$Rs?***

*Radioligand binding studies* - To evaluate whether the identified mRNA species for the 6TM-r$H_3$ isoforms code for functional $H_3$Rs, we transfected COS-7 cells with the cDNA encoding either the r$H_{3A}$R or one of the 6TM-r$H_3$ isoforms and evaluated corresponding membrane preparations for their ability to bind either the inverse $H_3$R agonist radioligand $^{125}$IPP or the $H_3$R agonist radioligand [$N^{\alpha}$-methyl-$^3$H]histamine. Cell homogenates derived from cells expressing the r$H_{3A}$R bind $^{125}$IPP with high affinity ($K_D$ = 2.1 nM, $B_{max}$ = 2.5 pmol/mg protein) and exhibits the expected affinities for IPP, immepip, and thioperamide ($pK_b$ for $^{125}$IPP 8.2±0.1, $pK_i$ values for immepip and thioperamide 6.5±0.2 and 7.7±0.1, respectively). In contrast, we failed to detect specific $^{125}$IPP-binding to cells transfected with cDNAs coding for any of the 6TM-r$H_3$ isoforms (Figure 3A). Similarly, we did not detect [$N^{\alpha}$-methyl-$^3$H]histamine binding to membranes of cells transfected with cDNAs encoding the 6TM-r$H_3$ isoforms (data not shown).

*Functional assays* – The $H_3$R couples to members of the $G_{i/o}$ family of G-proteins to inhibit adenylyl cyclase (AC) activity and subsequently inhibits the formation of intracellular cyclic AMP (cAMP) (Leurs et al., 2005). Co-transfection of COS-7 cells with the r$H_{3A}$R encoding

Molecular Pharmacology Fast Forward. Published on January 13, 2006 as DOI: 10.1124/mol.105.019299
This article has not been copyedited and formatted. The final version may differ from this version.



cDNA together with pTLN121CRE, a cAMP responsive element binding protein (CREB)-responsive firefly-luciferase reporter gene, allowed us to monitor $H_3R$-induced modulation of forskolin-induced reporter-gene expression. In concert with the $G_{i/o}$-coupled nature of the $H_3R$ (see Leurs et al., 2005), treatment of co-transfected cells with varying concentrations of the $H_3R$ agonists immepip, R(α)-methylhistamine, and histamine results in the dose dependent inhibition of 10 μM forskolin-induced firefly-luciferase expression by approximately 60% with $EC_{50}$ values of approx. 2, 7, and 43 nM, respectively (Figure 3B), in $rH_{3A}R$-expressing cells. Under these assay conditions we do not observe constitutive activity for the $rH_{3A}R$ as the inverse $H_3R$ agonist thioperamide (Leurs et al., 2005) is without effect on the forskolin-induced luciferase expression (Figure 3C). While 1μM R(α)-methylhistamine potently induces signalling via the $rH_{3A}R$, under the same assay conditions, R(α)-methylhistamine is without effect on the forskolin-induced firefly-luciferase expression in cells co-transfected with cDNAs encoding the reporter gene and either of the 6TM-$rH_3$ isoforms (Figure 3D).

***Is there a role for the 6TM-$rH_3$ isoforms?***

*Detection of epitope-tagged $rH_3R$ isoforms in co-expression studies* - The immunological and immunocytochemistry data obtained with the N-terminally HA-tagged HA-$rH_{3D}$ isoform indicates poor plasma membrane expression of the $rH_{3D}$ isoform (Figures 2E and 2F). In addition, in cells transfected with cDNA encoding either of the 6TM-$rH_3$ isoforms we have been unable to detect *i*) specific $^{125}$IPP or [$N^{\alpha}$-methyl-$^3$H]histamine binding (Figure 3A); *ii*) modulation of forskolin-induced transcriptional events that are otherwise modulated by $rH_{3A}R$ activation under the same conditions. In recent years accumulating evidence suggests that some GPCRs, e.g. the $GABA_B$ receptors (White et al., 1998) and odorant receptors (Hague et al.,

Molecular Pharmacology Fast Forward. Published on January 13, 2006 as DOI: 10.1124/mol.105.019299
This article has not been copyedited and formatted. The final version may differ from this version.



2004a), require particular protein-protein interactions to allow proper plasma membrane expression. As it seems that the 6TM-r$H_3$ isoforms are retained intracellularly, we therefore postulated that the additional expression of GPCRs may aid the cell surface expression of the 6TM-r$H_3$ isoforms. Conversly, the 6TM-r$H_3$ isoforms may possibly retain the co-expressed GPCRs intracellularly by acting as dominant negatives.

*Do the 6TM-r$H_3$ isoforms interfere with cell surface expression of 7TM-r$H_3$Rs?* – We co-tranfected COS-7 cells with the cDNAs coding for the HA-r$H_{3A}$R and the r$H_{3D}$ isoform. Similar to the effects of co-expression of alternative splice variants of human $\alpha_{1A}$-adrenoceptors (Cogé et al., 1999), we found that the co-expression of the r$H_{3D}$ isoform reduced the expression of the HA-r$H_{3A}$R at the plasma membrane. This phenomenon is observed using either an ELISA assay on intact cells or by applying immunocytochemistry techniques using a rhodamine labelled anti-HA antibody (Figures 4A and 4B, respectively).

*Evaluation of ligand-binding sites upon co-expression of 7TM-$H_3$R and 6TM-r$H_3$ isoforms* – To evaluate whether the loss of HA-r$H_{3A}$R-derived immunofluorescence at the cell surface upon co-expression of the r$H_{3D}$ isoform also results in a loss of ligand binding sites for $H_3$R ligands we performed radioligand binding assays. As shown in Figure 3A, $^{125}$IPP binding sites are detected upon the expression of 7TM-r$H_3$Rs (Drutel et al., 2001), such as the r$H_{3A}$R, whereas expression of the 6TM-r$H_3$ isoforms does not result in the formation of $^{125}$IPP binding sites.

The transfection of 0.25 μg/$10^6$ cells of cDNA coding for the r$H_{3A}$R resulted in the expression of 2.5 pmol/mg protein $^{125}$IPP binding sites. Co-expression of the r$H_{3A}$R together with the r$H_{3D}$ isoform, however, resulted in an r$H_{3D}$-isoform gene-dosage dependent reduction of r$H_{3A}$R-

Molecular Pharmacology Fast Forward. Published on January 13, 2006 as DOI: 10.1124/mol.105.019299
This article has not been copyedited and formatted. The final version may differ from this version.



derived $^{125}$IPP binding sites (Figure 5A); the remaining $^{125}$IPP binding sites exhibit a pharmacological indistinguishable from that of the $rH_{3A}R$ ($pK_b$ for $^{125}$IPP 8.1±0.1, $pK_i$ values for immepip and thioperamide 6.9±0.2 and 7.6±0.1, respectively). The co-expression of the $rH_{3E}$ or $rH_{3F}$ isoform together with the $rH_{3A}R$ resulted in a similar reduction of $^{125}$IPP binding sites (Figures 5B and 5C, respectively), indicating that the 6TM-$rH_3$ isoforms interfere with the expression of the $rH_{3A}R$. The maximal inhibition of $^{125}$IPP binding sites, as evaluated by a transfection of cells with an $rH_{3A}R$ : 6TM-$rH_3$ isoform cDNA ratio of 1:10, is ~ 50-75% (Figures 5A, 5B, and 5C). To evaluate whether the observed inhibition of $^{125}$IPP binding-site expression is specific for the 6TM-$rH_3$ isoforms, we performed additional experiments in which we co-transfected cells with the same amount of $rH_{3A}R$ cDNA in combination with various amounts of cDNA encoding the human histamine $H_1$ receptor ($hH_1R$) (Figure 5D). While the transfection of COS-7 cells with the $hH_1R$ cDNA resulted in the formation of binding-sites for the $H_1R$ radioligand [$^3$H]mepyramine with pharmacological characteristics of the $hH_1R$ (data not shown), no specific $^{125}$IPP binding was detected in $hH_1R$ expressing cells (Figure 5D). Co-transfection of cells with cDNAs encoding both the $rH_{3A}R$ and the $hH_1R$, however, did not influence the formation of $^{125}$IPP binding sites.

Similarly to the findings with the $hH_1R$, expression of the rat $H_2R$ ($rH_2R$) or the viral chemokine receptor from Karposi´s Sarcoma herpes virus KSHV-GPCR (also known as ORF74) in COS-7 cells resulted in the formation of binding sites for the $H_2R$ radioligand $^{125}$IAPT and $^{125}$I-CXCL8, a radioligand for ORF74, respectively, but not in the formation of $^{125}$IPP binding sites. Co-expression of the $rH_{3A}R$ with either the $rH_2R$ or ORF74, however, did not affect the formation of $rH_{3A}R$-derived $^{125}$IPP binding sites (Figure 5E).

Molecular Pharmacology Fast Forward. Published on January 13, 2006 as DOI: 10.1124/mol.105.019299
This article has not been copyedited and formatted. The final version may differ from this version.



We also evaluated the effects of the co-expression of the $rH_{3B}R$ and $rH_{3C}R$ with the $rH_E$ and $rH_F$ isoforms, respectively, on the formation of $^{125}$IPP binding sites. Similar to the expression of the $rH_{3A}R$, expression of the $rH_{3B}R$ or $rH_{3C}R$ in COS-7 cells results in the formation of $^{125}$IPP binding sites (Drutel et al., 2001). Co-expression of the $rH_{3B}R$ or $rH_{3C}R$ together with either the $rH_{3E}$ or $rH_{3F}$ isoform resulted in an $rH_{3E}$- and $rH_{3F}$-isoform gene-dosage dependent reduction of $rH_{3B}R$- (Figure 5F) and $rH_{3C}R$- (Figure 5G) derived $^{125}$IPP binding sites, respectively. The maximal inhibition of $^{125}$IPP binding sites, as evaluated by a transfection of cells with an $rH_{3B}R$ or $rH_{3C}R$ : 6TM-$rH_3$ isoform cDNA ratio of 1:10, is ~ 50-75% (Figures 5F and 5G), similar to our findings on the co-expression of the $rH_{3A}R$ with the 6TM-$rH_3$ isoforms (Figures 5A, 5B, and 5C).

Whilst the co-expression of the $rH_{3A}R$ with the $rH_{3D}$ isoform inhibits the formation of $^{125}$IPP binding sites, the remaining $^{125}$IPP binding sites exhibit unchanged pharmacological characteristics of the $rH_{3A}R$, as evidenced by its unchanged affinity for IPP (Figure 5H).

Collectively, these radioligand-binding data clearly demonstrate that the expression of the 6TM-$rH_3$ isoforms selectively interferes with the expression of the 7TM-$rH_3$Rs.

***Evaluation of $H_3$R-ligand induced [$^{35}$S]GTPγS binding upon co-expression of 7TM-$H_3$R and 6TM-$rH_3$ isoforms.***

*Creation of $rH_{3A}R$-Gα fusion proteins* – Since we failed to detect $H_3$R-agonist mediated [$^{35}$S]GTPγS binding to activated Gα proteins in cell membranes derived from 6TM-$rH_3$ isoform expressing cells (data not shown), we chose to evaluate $H_3$R-agonist induced [$^{35}$S]GTPγS binding to assess the effects of the co-expression of 6TM-$rH_3$ isoforms on the functionality of 7TM-$rH_3$Rs. To assess the effects of the co-expression of 6TM-$rH_3$ isoforms on the functionality

Molecular Pharmacology Fast Forward. Published on January 13, 2006 as DOI: 10.1124/mol.105.019299
This article has not been copyedited and formatted. The final version may differ from this version.



of 7TM-r$H_3$Rs we chose to evaluate $H_3$R-agonist induced [$^{35}$S]GTPγS binding to activated Gα proteins. To increase the sensitivity of this assay (Milligan, 2000) we created fusion proteins consisting of the r$H_{3A}$R fused to one of the PTX insensitive mutant rat $G\alpha_{i/o}$ proteins: $G\alpha_{i1}C^{351}I$, $G\alpha_{i2}C^{352}I$, $G\alpha_{i3}C^{351}I$, or $G\alpha_oC^{351}I$ (creating r$H_{3A}$R-$G\alpha_{o1}C^{351}I$, r$H_{3A}$R-$G\alpha_{i1}C^{351}I$, r$H_{3A}$R-$G\alpha_{i2}C^{352}I$, and r$H_{3A}$R-$G\alpha_{i3}C^{351}I$, respectively) by PCR according to Methods.

*Characterisation of r$H_{3A}$R-Gα fusion proteins* - The four different r$H_{3A}$R fusion proteins r$H_{3A}$R-$G\alpha_{o1}C^{351}I$, r$H_{3A}$R-$G\alpha_{i1}C^{351}I$, r$H_{3A}$R-$G\alpha_{i2}C^{352}I$, and r$H_{3A}$R-$G\alpha_{i3}C^{351}I$, were subsequently characterised by $^{125}$IPP binding assays upon their heterologous expression in COS-7 cells. Based on these studies (data not shown) we decided to continue our experiments using the r$H_{3A}$R-$G\alpha_{o1}C^{351}I$ fusion protein as this fusion protein exhibited a $pK_b$ value for $^{125}$IPP of 8.4 ± 0.2 that corresponds to the obtained $pK_b$ value of $^{125}$IPP for the wild-type r$H_{3A}$R of 8.2 ± 0.1. Also, the affinities of the wild-type r$H_{3A}$R and the r$H_{3A}$R-$G\alpha_{o1}C^{351}I$ fusion protein for the $H_3$R agonist immepip and the inverse $H_3$R agonist thioperamide are similar (6.5±0.2 and 7.7±0.1 *versus* 6.9±0.1 and 7.9±0.1, respectively).

Subsequently we compared the capability of the r$H_{3A}$R-$G\alpha_{o1}C^{351}I$ fusion protein to mediate the inhibition of 10μM forskolin-induced activation of CRE-mediated gene transcription in COS-7 cells. We found the the r$H_{3A}$R-$G\alpha_{o1}C^{351}I$ fusion protein to potently inhibit the forskolin-induced response upon activation with $H_3$R agonists. In concert with our findings on the wild-type r$H_{3A}$R, treatment of cells co-transfected with cDNAs encoding the r$H_{3A}$R-$G\alpha_{o1}C^{351}I$ fusion protein and the CRE-reporter gene with varying concentrations of the $H_3$R agonists immepip, R(α)-methylhistamine, and histamine results in the dose dependent inhibition of 10 μM forskolin-induced firefly-luciferase expression by approximately 40% with $EC_{50}$ values of approx. 4, 30,

Molecular Pharmacology Fast Forward. Published on January 13, 2006 as DOI: 10.1124/mol.105.019299
This article has not been copyedited and formatted. The final version may differ from this version.



and 76 nM, respectively (Figure 6A).These data indicate that the $rH_{3A}R$-$G\alpha_{o1}C^{351}I$ fusion protein is fully functional and shows a $rH_{3A}R$ pharmacology.

*Co-expression of $rH_{3A}R$-$G\alpha_{o1}C^{351}I$ fusion proteins and the $rH_{3D}$ isoform* - Consistent with our findings on the co-expression of 7TM-$rH_{3A}$Rs with the 6TM-$rH_3$ isoforms (see Figure 5), co-expression of the $rH_{3A}R$-$G\alpha_{o1}C^{351}I$ fusion protein together with the $rH_{3D}$ isoform, results in an $rH_{3D}$-isoform gene-dosage dependent reduction of $rH_{3A}R$-$G\alpha_{o1}C^{351}I$ fusion protein -derived $^{125}$IPP binding sites (Figure 6B), and the remaining $^{125}$IPP binding sites exhibit an $rH_{3A}R$-$G\alpha_{o1}C^{351}I$-like pharmacological profile ($pK_b$ for $^{125}$IPP 8.5±0.1, $pK_i$ values for immepip and thioperamide 7.0±0.2 and 7.6±0.1, respectively). The maximal inhibition of $rH_{3A}R$-$G\alpha_{o1}C^{351}I$-derived $^{125}$IPP binding sites, as evaluated by a transfection of cells with an $rH_{3A}R$-$G\alpha_{o1}$ : $rH_{3D}$ isoform cDNA ratio of 1:10, is ~ 65% (Figure 6B).

We subsequently assessed the influence of co-expression of the $rH_{3D}$ isoform on the [$^{35}$S]GTPγS binding induced by agonist-mediated activation of co-expressed $rH_{3A}R$-$G\alpha_{o1}C^{351}I$ fusion proteins. The $H_3R$ agonist immepip (1 μM) resulted in a robust stimulation of [$^{35}$S]GTPγS binding in $rH_{3A}R$-$G\alpha_{o1}C^{351}I$ expressing cells, that was inhibited by co-incubation with 1 μM of the inverse $H_3R$ agonist thioperamide (Figure 6C). Under the assay conditions used, we could not detect significant thioperamide-mediated inhibition of basal $rH_{3A}R$-$G\alpha_{o1}C^{351}I$ mediated [$^{35}$S]GTPγS binding, indicating that we could not detect constitutive $rH_{3A}R$-$G\alpha_{o1}C^{351}I$ activity. The 1 μM immepip-induced [$^{35}$S]GTPγS binding was inhibited by 70 % by co-expression of the $rH_{3A}R$-$G\alpha_{o1}C^{351}I$ fusion protein with the $rH_{3D}$ isoform (Figure 6C). The 6TM-$rH_3$ isoforms

Molecular Pharmacology Fast Forward. Published on January 13, 2006 as DOI: 10.1124/mol.105.019299
This article has not been copyedited and formatted. The final version may differ from this version.



themselves did not mediate changes in [$^{35}$S]GTPγS binding upon incubation with $H_3R$ ligands (data not shown).

***Can $rH_3Rs$ form homo-oligomers?***

In view of the emerging concept of GPCR dimerisation that is now well documented in literature (see e.g. Pfleger and Eidne, 2005 for a review), we speculated that the 6TM-$rH_3$ isoforms might interfere with the cell surface expression of 7TM-$rH_3$ receptors through dimerisation.

Previously we described the generation of anti-$rH_{3C}$ 268-277Cys antibodies (Shenton et al., 2005), which based on immunoblotting, selectively recognize both the $rH_{3A}R$ and $rH_{3C}R$ isoform, but not the $rH_{3B}R$ isoform expressed in HEK 293 cells. Wild-type $rH_{3A}R$ expressing cells were collected and subjected to crosslinking with varying amounts of the cell permeable cross-linker bis(sulfosuccinimidyl)suberate (BS3) prior to resolving the samples using SDS-PAGE. Immunoblotting with anti-$H_{3C}$ 268-277Cys antibody yielded three major protein species ($M_r$ 90,000, $M_r$ 135,000 and approx. Mr 200,000, respectively), corresponding well to putative dimeric, trimeric and tetrameric $rH_{3A}R$ oligomers, respectively (Figure 7, lanes 1-3). Performing similar experiments using native rat brain tissue, the major species observed is a coincident $M_r$ 90,000 species (Figure 7, lane 4). Interestingly, a recombinant putative monomeric $M_r$ 47,000 species was clearly observed, which was barely detectable in the native forebrain preparation. Higher crosslinker concentrations yielded >200,000 species for both recombinant and native $H_3R$ preparations (Shenton et al., 2005).

We have previously successfully used the *time-resolved* Fluorescent Resonance Energy Transfer (*tr*-FRET) fluorescence (665-nm emission after excitation at 320 nm) for the detection of $hH_1R$

Molecular Pharmacology Fast Forward. Published on January 13, 2006 as DOI: 10.1124/mol.105.019299
This article has not been copyedited and formatted. The final version may differ from this version.



dimerisation using epitope tagged $hH_1Rs$ and fluorescently labeled antibodies recognizing the N-terminally epitope-tagged receptors (Bakker et al., 2004a). We have used this approach to confirm the formation of oligomerisation of $rH_3Rs$.

*tr*-FRET fluorescence results obtained with the different samples are shown in Figure 7B. A clear specific *tr*-FRET signal is observed using live cells expressing the HA-$rH_{3A}Rs$. The data is presented as the *tr*-FRET that is observed using HA-$rH_{3A}R$ expressing cells that have been incubated with both anti-HA-$Eu^{3+}$ and anti-HA-allophycocyanin antibodies *versus* the *tr*-FRET that is observed using a mix of two populations of HA-$rH_{3A}R$ expressing cells that proir to mixing were independently incubated with with either of the two antibodies.The increased *tr*-FRET signal can only be explained due to the resonance energy transfer from anti-HA-$Eu^{3+}$ antibodies bound to HA-$rH_{3A}Rs$ to anti-HA-allophycocyanin antibodies bound to HA-$rH_{3A}Rs$, indicative of the formation of $rH_{3A}R$ multimers in living cells.

***Modulation of $rH_{3AD}$ and $rH_{3DEF}$ isoform-specific mRNAs in rat brain after delivery of a systemic convulsant.***

Previously we have successfully used specific oligonucleotide probes to characterise the 7TM-$rH_3R$ mRNA expression in the rat brain (Drutel et al., 2001). To evaluate the CNS expression of the 6TM-$rH_3$ isoforms we have designed domain specific probes. We have used one probe specific for the C-terminus present in the 6TM-$rH_3$ isoforms, and, as a comparison, we have also performed studies using a oligonucleotide probe specific for the (full length) third intracellular loop of the $rH_{3A}R$, which is also present in the $rH_{3D}$ isoform (but not any of the other $rH_3$ isoforms identified to date; Figure 8A).

Molecular Pharmacology Fast Forward. Published on January 13, 2006 as DOI: 10.1124/mol.105.019299
This article has not been copyedited and formatted. The final version may differ from this version.



Significant increases in mRNA expression levels of $H_3R$ isoforms with full length third intracellular loop (detected using probe $H_{3AD}$) were observed in layers II-VIb of cortex (48h post-injection), caudate putamen (48h post-injection), piriform cortex (48h post-injection), and CA1 region of the hippocampus (24h post-injection) (Figure 8B) after PTZ. Figure 8C illustrates mRNA expression levels and differences for $H_{3A}$ and $H_{3D}$ isoforms in representative sections from control and 48h post-injection animals.

In contrast, decreases in mRNA expression pattern of 6TM-r$H_3$ isoforms (detected using probe $H_{3DEF}$) were observed in layers II-VIb of cortex (6h post-injection), piriform cortex (6h, 24h, and 48h post-injection), CA1 region of the hippocampus (24h post-injection), and CA3 region of the hippocampus (24h post-injection) (Figure 8D). Figure 8E shows mRNA expression patterns and differences for 6TM-r$H_3$ isoforms in representative sections from control and 24h post-injection animals.

## DISCUSSION

Our search for additional alternative splice variants of the $rH_3R$ resulted in the identification of three mRNAs coding for heretofore uncharacterised $rH_3$ isoforms. In contrast to the known functional $H_3Rs$, sequence analysis of these newly identified isoforms reveals that an additional splicing event occurs within a region corresponding to TM6, resulting in isoforms with an alternative C-terminal domain and isoforms that are predicted to possess only 6 TMs. The mRNAs encoding these 6TM-$rH_3$ isoforms are expressed in the rat brain with a distribution pattern that is similar to the previously identified functional 7TM-$rH_3Rs$ (Drutel et al., 2001). While there may be differences in the rate of synthesis, the inherent stability, and the rate of degradation of the various $H_3$ isoforms resulting in differences in their expression levels, extensive analysis of the 6TM-$rH_3$ isoforms through heterologous expression studies, however, failed to identify any ligand-binding and functional signalling events modulated by these 6TM-$rH_3$ isoforms. The 6TM-$rH_3$ isoforms appear to be localized intracellulary, and succeeding studies revealed the ability of the 6TM-$rH_3$ isoforms to interfere with the cell surface expression and subsequent signalling of the previously identified 7TM-$rH_3$ isoforms, thus acting as dominant negatives.

An increasing number of GPCRs have been shown to exist as oligomeric complexes (see e.g. Pfleger and Eidne, 2005 for a review), which are thought to be formed early during biosynthesis (Terrillon et al., 2003). In this study we show that also the $rH_{3A}R$ is present as dimers or higher order oligomeric complexes both in transfected cells an in rat brain. The oligomerization of GPCRs during biosynthesis and maturation appears crucial for proper exportation of receptors to

Molecular Pharmacology Fast Forward. Published on January 13, 2006 as DOI: 10.1124/mol.105.019299
This article has not been copyedited and formatted. The final version may differ from this version.



the plasma membrane (reviewed in Bulenger et al., 2005). The co-expression and formation of heterodimeric $\beta_2$-ARs (Hague et al., 2004a) aids for instance the cell surface trafficking of olfactory GPCRs that are otherwise retained and degraded in the ER (Lu et al., 2003; Lu et al., 2004), as well as of the $\alpha_{1D}$-AR that normally is trafficked poorly to the cell surface (Uberti et al., 2004). The co-expression of differentially spliced GPCR variants may also aid the cell-surface expression, as shown for instance by the co-expression of the $\alpha_{1D}$-AR with $\alpha_{1B}$-ARs (Hague et al., 2004b). In contrast, certain alternatively spliced variants of for instance the $\alpha_{1A}$-AR (Cogé et al., 1999), the calcitonin receptor (Seck et al., 2003) and the dopamine $D_3$ receptor (Karpa et al., 2000) appear to dimerise with their cognate full-length receptors and impede their cell surface expression due to mislocalization to an intracellular compartment. The co-expression of the herein described 6TM-r$H_3$ isoforms not only reduced cell surface expression of the 7TM-r$H_3$Rs, but consequently also resulted in a reduced 7TM-r$H_3$R mediated signalling. Our data are therefore consistent with the reported findings on the co-expression of N-terminal truncated, dominant negative mutants and wild-type $V_2$ receptors, which results in the formation of heterodimers and reduced agonist binding, signal transduction and cell-surface trafficking of the full-length $V_2$ receptor (Zhu and Wess, 1998). Similar to our findings on the 6TM-r$H_3$ isoforms, mutants of the $\alpha_2$-AR (Zhou et al.), vasopressin $V_2$ (Zhu and Wess, 1998), dopamine $D_2$ (Lee et al., 2000), chemokine receptor CCR5 (Benkirane et al., 1997; Blanpain et al., 2000; Chelli and Alizon, 2001), gonadotropin-releasing hormone (GnRH) receptor (Brothers et al., 2004), and the platelet-activating factor (Le Gouill et al., 1999) receptors also impede the cell surface expression of their co-expressed wild-type counterparts, thus exhibiting *trans*-dominant negative effects on wild-type receptor expression (Benkirane et al., 1997; Brothers et al., 2004; Chelli and Alizon, 2001), most likely through dimerization. It appears most likely that the 6TM-r$H_3$

Molecular Pharmacology Fast Forward. Published on January 13, 2006 as DOI: 10.1124/mol.105.019299
This article has not been copyedited and formatted. The final version may differ from this version.



isoforms interfere with the functional expression of the 7TM-r$H_3$Rs through hetero-dimerization. Although direct hetero-dimerization of the 6TM-r$H_3$ isoforms with the 7TM-r$H_3$Rs remains to be established, we have shown the r$H_{3A}$R to be constitutively expressed as a dimeric receptor in the brain as well as upon heterologous expression.

GPCRs have been found to interact with accessory proteins which can be critical for their biogenesis (see also Bermak and Zhou, 2001 for a review; Metherell et al., 2005). A conserved F$(X)_6$LL motif, which is suggested to be important for the proper GPCR folding and subsequent export from the ER (Duvernay et al., 2004), is also present in the C-terminal domain of the 7TM-r$H_3$Rs, but is lacking in the 6TM-r$H_3$ isoforms. Mutations in regions overlapping the F$(X)_6$LL motif in the dopamine $D_1$ receptor resulted in ER retention of the mutant receptor and loss of cell surface expression, and subsequent studies revealed that this region is important for a interactions with a specific ER-membrane-associated protein that regulates transport of GPCRs (Bermak et al., 2001). Intriguingly, instead of the F$(X)_6$LL motif, the 6TM-r$H_3$ isoforms possess an RXR ER retention signal. Collectively, these data suggest that the 6TM-r$H_3$ isoforms lack protein-protein interactions with specific accessory proteins in the ER that are required for cell-surface expression. Although the localisation of the 6TM-r$H_3$ isoforms within the ER appears likely, this needs to be verified by future experiments. Nonetheless, the findings on GPR30 as an intracellular GPCR (Revankar et al., 2005) points out that the 6TM-r$H_3$ isoforms may well have yet undiscovered intracellular functions in addition to their capability to retain the 7TM-r$H_3$Rs intracellularly.

On the one hand, the 6TM-r$H_3$ splice varients may act as 'antichaperones' inhibiting specific chaperones' activities or preventing their access to the 7TM-r$H_3$Rs. Alternatively, the association of the 6TM-r$H_3$ isoforms with the 7TM-r$H_3$R isoforms in the ER may actively unfold or result in

Molecular Pharmacology Fast Forward. Published on January 13, 2006 as DOI: 10.1124/mol.105.019299
This article has not been copyedited and formatted. The final version may differ from this version.



the misfolding of the protein complex. As we find the $rH_{3D}$ isoform not to interfere with the cell surface expression of unrelated GPCRs, it seems unlikely the 6TM-$rH_3$ isoforms act through blocking either the ER or Golgi, or to promote ER-associated protein degradation. The precise mechanism underlying the action of the newly identified isoforms, however, remains unkown. Our data suggests that the regulation of the alternative $rH_3R$ mRNA splicing is a new and effective means for the regulation of $H_3R$ signalling. Functional (including constitutive) $H_3R$ activity may be regulated through the regulation of the splicing-events underlying the occurrence of the various $H_3R$ isoforms. Interestingly, several cell signalling pathways, including the MAPK pathway, regulate mRNA splicing (reviewed in Shin and Manley, 2004). Intriguingly, the $H_3R$ activates the MAPK pathway (Drutel et al., 2001; Giovannini et al., 2003), arguing for the possibility of activation of splicing factors and hence, an autoregulation of the $H_3R$ activity.

Our studies also show that the expression pattern of the 7TM-$rH_3Rs$ and the 6TM-$rH_3$ isoforms overlaps substantially in rat brain. Moreover, PTZ-induced seizures result in suppression of 6TM-$rH_3$ (probe $H_{3DEF}$) isoform mRNAs in particular brain regions while mRNA levels of the isoforms with the full third intracellular loop (probe $H_{3AD}$) are increased. A characteristic transient and short-living increase in the mRNA for the full-length third intracellular loop (probe $H_{3AD}$), hippocampal $CA_{3c}$ area, followed by piriform cortex, amygdala and hippocampal $CA_1$ area is observed after systemic injection of kainic acid, a model of temporal lobe epilepsy (Lintunen et al., 2005), indicating a spatiotemporal correlation to progressing neuronal damage in this model of temporal epilepsy. Previous studies on PTZ have indicated damaged neurons in the rostral limbic cortex (both the orbital, agranular insular and pre-limbic), the lateral hypothalamus (in the vicinity of the rostral medial forebrain bundle), the bed nucleus of the stria

Molecular Pharmacology Fast Forward. Published on January 13, 2006 as DOI: 10.1124/mol.105.019299
This article has not been copyedited and formatted. The final version may differ from this version.



terminalis, the claustrum, the hippocampal formation (CA3 and entorhinal cortex) and lateral thalamic nuclei 50 min post injection (Ben-Ari et al., 1981). The increases in $H_3R$ mRNA with full third intracellular loop as observed in this study after PTZ were observed significantly later than the reported damage begins (Ben-Ari et al., 1981), in agreement with the concept that the mechanisms of neuronal damage following kainic acid and PTZ are different. Although the piriform cortex has not been reported to suffer significant damage after PTZ (Ben-Ari et al., 1981), it seems not to be only a primary sensory area but because of its neuronal organization and associative fiber system may also be involved in the pathological mechanisms leading to seizures (Löscher and Ebert, 1996). Of the areas studied here, the piriform cortex showed a sustained decline in 6TM-r$H_3$ mRNA expression. Interestingly, we observed a significant transient increase in $H_3R$ radioligand binding in piriform cortex at 6 h after PTZ concomitantly with the decline of $H_{3DEF}$ isoform mRNAs (data not shown). However, a similar strong correlation was not found in all areas where smaller changes were seen, suggesting that other factors in addition to mRNA ratios may affect receptor binding. The high susceptibility for induction of seizures by chemical or electrical stimulation and various studies addressing its role in seizure generation suggest that the piriform cortex can also function as an amplifier region to increase and propagate seizure activity induced in other limbic regions (Löscher and Ebert, 1996). Increased $H_3R$ activity (e.g., expression and translation) in this region could result in decreased glutamate release (Brown and Haas, 1999; Molina-Hernandez et al., 2001), as glutamatergic neurons exist in the piriform cortex (Riba-Bosch and Perez-Clausell, 2004), for control of overall neuronal activity in the region.

The abundance of mRNA coding for the 6TM-r$H_3$ isoforms suggest that its production may have important biological implications. For example, in addition to its ability to interfere with cell

Molecular Pharmacology Fast Forward. Published on January 13, 2006 as DOI: 10.1124/mol.105.019299
This article has not been copyedited and formatted. The final version may differ from this version.



surface expression of functional $rH_3Rs$, which may arise from modification of the stability of the mRNA encoding functional 7TM-$rH_3Rs$, the 6TM-$rH_3$ isoform mRNAs might encode proteins with yet unidentified functions. Further analysis of the alternatively spliced products of the $H_3R$ gene is required to elucidate their biological significance.

In conclusion, we have identified three additional splice variants of the $rH_3R$. The mRNAs of these isoforms are abundantly expressed in the brain and the expression pattern largely overlaps with that of the known $rH_{3A-C}R$ isoforms. Analysis of the sequence of these $rH_{3D}$, $rH_{3E}$, and $rH_{3F}$ isoforms reveals these isoforms to consist of 6TM domains. The 6TM-$rH_3$ isoforms are retained intracellularly upon heterologous expression, and in subsequent pharmacological analysis studies we could not detect any ligand binding or functional activity for these 6TM-$rH_3$ isoforms. The 6TM-$rH_3$ isoforms, however, selectively impede cell surface expression of the functional 7TM-$rH_3Rs$. Moreover, the mRNA levels of the $rH_3$ isoforms in rat brain are modulated by treatment with the convulsant PTZ. Although, the functional significance and possible roles of these 6TM-$rH_3$ isoforms in (patho-)physiology remain to be established, these findings provide novel insight in the regulation of the histaminergic system in the brain.

Molecular Pharmacology Fast Forward. Published on January 13, 2006 as DOI: 10.1124/mol.105.019299
This article has not been copyedited and formatted. The final version may differ from this version.



## ACKNOWLEDGMENTS

This paper is dedicated to Dr. Art A. Hancock, who sadly passed away in November last year. Dr. Hancock was a great scientist with a warm and generous personality. Under his inspired leadership Abbott Laboratories has made many seminal contributions to the field of $H_3$ receptors. We thank Sarina M. Meusburger, Franca di Summa, Kim Retra, and José Antonio Arias-Montaño for expert assisance.

## REFERENCES

Bakker RA (2004) Histamine $H_3$-receptor isoforms. *Inflamm Res* **53**(10):509-516.

Bakker RA, Dees G, Carrillo JJ, Booth RG, López-Gimenez JF, Milligan G, Strange PG and Leurs R (2004a) Domain swapping in the human histamine $H_1$ receptor. *J Pharmacol Exp Ther* **311**:131-138.

Bakker RA, Weiner DM, ter Laak T, Beuming T, Zuiderveld OP, Edelbroek M, Hacksell U, Timmerman H, Brann MR and Leurs R (2004b) 8*R*-lisuride is a potent stereospecific histamine $H_1$-receptor partial agonist. *Mol Pharmacol* **65**(3):538-549.

Ben-Ari Y, Tremblay E, Riche D, Ghilini G and Naquet R (1981) Electrographic, clinical and pathological alterations following systemic administration of kainic acid, bicuculline or pentetrazole: metabolic mapping using the deoxyglucose method with special reference to the pathology of epilepsy. *Neuroscience* **6**(7):1361-1391.

Benkirane M, Jin DY, Chun RF, Koup RA and Jeang KT (1997) Mechanism of transdominant inhibition of CCR5-mediated HIV-1 infection by ccr5Δ32. *J Biol Chem* **272**(49):30603-30606.

Bermak JC, Li M, Bullock C and Zhou QY (2001) Regulation of transport of the dopamine D1 receptor by a new membrane-associated ER protein. *Nat Cell Biol* **3**(5):492-498.

Bermak JC and Zhou QY (2001) Accessory proteins in the biogenesis of G protein-coupled receptors. *Mol Interv* **1**(5):282-287.

Blanpain C, Lee B, Tackoen M, Puffer B, Boom A, Libert F, Sharron M, Wittamer V, Vassart G, Doms RW and Parmentier M (2000) Multiple nonfunctional alleles of CCR5 are frequent in various human populations. *Blood* **96**(5):1638-1645.

Brothers SP, Cornea A, Janovick JA and Conn PM (2004) Human loss-of-function gonadotropin-releasing hormone receptor mutants retain wild-type receptors in the endoplasmic reticulum: molecular basis of the dominant-negative effect. *Mol Endocrinol* **18**(7):1787-1797.

Brown RE and Haas HL (1999) On the mechanism of histaminergic inhibition of glutamate release in the rat dentate gyrus. *J Physiol* **515 (Pt 3)**:777-786.

Bulenger S, Marullo S and Bouvier M (2005) Emerging role of homo- and heterodimerization in G-protein-coupled receptor biosynthesis and maturation. *Trends in Pharmacological Sciences* **26**(3):131-137.

Chazot PL, Hann V, Wilson C, Lees G and Thompson CL (2001) Immunological identification of the mammalian $H_3$ histamine receptor in the mouse brain. *Neuroreport* **12**(2):259-262.

Chelli M and Alizon M (2001) Determinants of the *trans*-dominant negative effect of truncated forms of the CCR5 chemokine receptor. *J Biol Chem* **276**(50):46975-46982.

Cogé F, Guénin SP, Audinot V, Renouard-Try A, Beauverger P, Macia C, Ouvry C, Nagel N, Rique H, Boutin JA and Galizzi JP (2001) Genomic organization and characterization of splice variants of the human histamine $H_3$ receptor. *Biochem J* **355**(Pt 2):279-288.

Cogé F, Guenin SP, Renouard-Try A, Rique H, Ouvry C, Fabry N, Beauverger P, Nicolas JP, Galizzi JP, Boutin JA and Canet E (1999) Truncated isoforms inhibit [$^3$H]prazosin binding and cellular trafficking of native human $\alpha_{1A}$-adrenoceptors. *Biochem J* **343 Pt 1**:231-239.

Drutel G, Peitsaro N, Karlstedt K, Wieland K, Smit MJ, Timmerman H, Panula P and Leurs R (2001) Identification of rat $H_3$ receptor isoforms with different brain expression and signaling properties. *Mol Pharmacol* **59**(1):1-8.

Duvernay MT, Zhou F and Wu G (2004) A conserved motif for the transport of G protein-coupled receptors from the endoplasmic reticulum to the cell surface. *J Biol Chem* **279**(29):30741-30750.

Giovannini MG, Efoudebe M, Passani MB, Baldi E, Bucherelli C, Giachi F, Corradetti R and Blandina P (2003) Improvement in fear memory by histamine-elicited ERK2 activation in hippocampal CA3 cells. *J Neurosci* **23**(27):9016-9023.

Hague C, Uberti MA, Chen Z, Bush CF, Jones SV, Ressler KJ, Hall RA and Minneman KP (2004a) Olfactory receptor surface expression is driven by association with the $\beta_2$-adrenergic receptor. *Proc Natl Acad Sci U S A* **101**(37):13672-13676.

Hague C, Uberti MA, Chen Z, Hall RA and Minneman KP (2004b) Cell surface expression of $\alpha_{1D}$-adrenergic receptors is controlled by heterodimerization with $\alpha_{1B}$-adrenergic receptors. *J Biol Chem* **279**(15):15541-15549.

Hawrylyshyn KA, Michelotti GA, Coge F, Guenin SP and Schwinn DA (2004) Update on human alpha1-adrenoceptor subtype signaling and genomic organization. *Trends Pharmacol Sci* **25**(9):449-455.

Karpa KD, Lin R, Kabbani N and Levenson R (2000) The dopamine D3 receptor interacts with itself and the truncated D3 splice variant d3nf: D3-D3nf interaction causes mislocalization of D3 receptors. *Mol Pharmacol* **58**(4):677-683.

Kilpatrick GJ, Dautzenberg FM, Martin GR and Eglen RM (1999) 7TM receptors: the splicing on the cake. *Trends Pharmacol Sci* **20**(7):294-301.

Le Gouill C, Parent JL, Caron CA, Gaudreau R, Volkov L, Rola-Pleszczynski M and Stankova J (1999) Selective modulation of wild type receptor functions by mutants of G-protein-coupled receptors. *J Biol Chem* **274**(18):12548-12554.

Lee SP, O'Dowd BF, Ng GY, Varghese G, Akil H, Mansour A, Nguyen T and George SR (2000) Inhibition of cell surface expression by mutant receptors demonstrates that D2 dopamine receptors exist as oligomers in the cell. *Mol Pharmacol* **58**(1):120-128.

Leurs R, Bakker RA, Timmerman H and de Esch IJ (2005) The histamine $H_3$ receptor: from gene cloning to $H_3$ receptor drugs. *Nat Rev Drug Discov* **4**(2):107-120.

Lintunen M, Sallmen T, Karlstedt K and Panula P (2005) Transient changes in the limbic histaminergic system after systemic kainic acid-induced seizures. *Neurobiol Dis* **20**(1):155-169.

Löscher W and Ebert U (1996) The role of the piriform cortex in kindling. *Prog Neurobiol* **50**(5-6):427-481.

Lu M, Echeverri F and Moyer BD (2003) Endoplasmic reticulum retention, degradation, and aggregation of olfactory G-protein coupled receptors. *Traffic* **4**(6):416-433.

Lu M, Staszewski L, Echeverri F, Xu H and Moyer BD (2004) Endoplasmic reticulum degradation impedes olfactory G-protein coupled receptor functional expression. *BMC Cell Biol* **5**(1):34.

Metherell LA, Chapple JP, Cooray S, David A, Becker C, Ruschendorf F, Naville D, Begeot M, Khoo B, Nurnberg P, Huebner A, Cheetham ME and Clark AJ (2005) Mutations in MRAP, encoding a new interacting partner of the ACTH receptor, cause familial glucocorticoid deficiency type 2. *Nat Genet* **37**(2):166-170.

Milligan G (2000) Insights into ligand pharmacology using receptor-G-protein fusion proteins. *Trends in Pharmacological Sciences* **21**(1):24-28.

Molina-Hernandez A, Nunez A, Sierra JJ and Arias-Montano JA (2001) Histamine $H_3$ receptor activation inhibits glutamate release from rat striatal synaptosomes. *Neuropharmacology* **41**(8):928-934.

Morisset S, Sasse A, Gbahou F, Héron A, Ligneau X, Tardivel-Lacombe J, Schwartz JC and Arrang JM (2001) The rat $H_3$ receptor: gene organization and multiple isoforms. *Biochem Biophys Res Commun* **280**(1):75-80.

Pfleger KD and Eidne KA (2005) Monitoring the formation of dynamic G-protein-coupled receptor-protein complexes in living cells. *Biochem J* **385**(Pt 3):625-637.

Revankar CM, Cimino DF, Sklar LA, Arterburn JB and Prossnitz ER (2005) A transmembrane intracellular estrogen receptor mediates rapid cell signaling. *Science* **307**(5715):1625-1630.

Riba-Bosch A and Perez-Clausell J (2004) Response to kainic acid injections: changes in staining for zinc, FOS, cell death and glial response in the rat forebrain. *Neuroscience* **125**(3):803-818.

Schmauss C, Haroutunian V, Davis KL and Davidson M (1993) Selective loss of dopamine $D_3$-type receptor mRNA expression in parietal and motor cortices of patients with chronic schizophrenia. *Proc Natl Acad Sci U S A* **90**(19):8942-8946.

Seck T, Baron R and Horne WC (2003) The alternatively spliced Δe13 transcript of the rabbit calcitonin receptor dimerizes with the C1a isoform and inhibits its surface expression. *J Biol Chem* **278**(25):23085-23093.

Shenton FC, Hann V and Chazot PL (2005) Evidence for native and cloned $H_3$ histamine receptor higher oligomers. *Inflammation Res* **54**:S48-S49.

Shin C and Manley JL (2004) Cell signalling and the control of pre-mRNA splicing. *Nat Rev Mol Cell Biol* **5**(9):727-738.

Smit MJ, Verzijl D, Casarosa P, Navis M, Timmerman H and Leurs R (2002) Kaposi's sarcoma-associated herpesvirus-encoded G protein-coupled receptor ORF74 constitutively activates p44/p42 MAPK and Akt via $G_i$ and phospholipase C-dependent signaling pathways. *J Virol* **76**(4):1744-1752.

Terrillon S, Durroux T, Mouillac B, Breit A, Ayoub MA, Taulan M, Jockers R, Barberis C and Bouvier M (2003) Oxytocin and vasopressin V1a and V2 receptors form constitutive homo- and heterodimers during biosynthesis. *Mol Endocrinol* **17**(4):677-691.

Uberti MA, Hague C, Oller H, Minneman KP and Hall RA (2005) Heterodimerization with $\beta_2$-adrenergic receptors promotes surface expression and functional activity of $\alpha_{1D}$-adrenergic receptors. *J Pharmacol Exp Ther* **313**(1):16-23.

White JH, Wise A, Main MJ, Green A, Fraser NJ, Disney GH, Barnes AA, Emson P, Foord SM and Marshall FH (1998) Heterodimerization is required for the formation of a functional $GABA_B$ receptor. *Nature* **396**(6712):679-682.

Zhou F, Filipeanu CM, Duvernay MT and Wu G (2006) Cell-surface targeting of $\alpha_2$-adrenergic receptors -- Inhibition by a transport deficient mutant through dimerization. *Cellular Signalling* **18**(3):318-327.

Zhu X and Wess J (1998) Truncated $V_2$ vasopressin receptors as negative regulators of wild-type $V_2$ receptor function. *Biochemistry* **37**(45):15773-15784.

Molecular Pharmacology Fast Forward. Published on January 13, 2006 as DOI: 10.1124/mol.105.019299
This article has not been copyedited and formatted. The final version may differ from this version.



FOOTNOTES

a) Unnamed footnotes:

* Financial support: *RL* is a recipient of a PIONIER award of the Technology Foundation (STW) of the Netherlands Foundation of Scientific Research (NWO). Supported by the Academy of Finland (*PP*), and the Finnish Foundation for Alcohol Studies (*PP*, *ML* and *AL*).

§ Current addresses: Boehringer Ingelheim Pharma GmbH & Co. KG, Department of Metabolic Diseases, 88397 Biberach, Germany (*RAB*); Galapagos Genomics BV, 2333 CN Leiden, The Netherlands (*MH*); and Institut François Magendie, 33077 Bordeaux cedex, MC Université Bx2, France (*GD*).

b) Reprint requests to: Dr. R. Leurs, Leiden/Amsterdam Center for Drug Research, Department of Medicinal Chemistry, Vrije Universiteit Amsterdam, De Boelelaan 1083, 1081HV Amsterdam, The Netherlands. Tel: ++31-20-5987600. Fax: ++31-20-5987610. E-mail: r.leurs@few.vu.nl.

c) Numbered footnotes: *none*.

Molecular Pharmacology Fast Forward. Published on January 13, 2006 as DOI: 10.1124/mol.105.019299
This article has not been copyedited and formatted. The final version may differ from this version.



FIGURE LEGENDS

Figure 1. Sequence alignment of $rH_3R$ isoforms and genomic organisation of the $rH_3R$ gene. *A*, Amino-acid sequence alignment of various $rH_3R$ isoforms.The $rH_{3B}R$ and $rH_{3C}R$ isoforms exhibit amino-acid deletions in the third intracellular loop of the $rH_3R$ protein compared to the full length $rH_{3A}R$. The $rH_{3D}$, $rH_{3E}$, and $rH_{3F}$ isoforms differ from the $rH_{3A}R$, $rH_{3B}R$ and $rH_{3C}R$ isoforms, respectively, in an alternative C-terminal domain as a result of an additional splicing event (see Figure 1*A*). Indicated above the amino acids are the seven transmembrane domains as they are found for the $rH_{3A}R$, $rH_{3B}R$ and $rH_{3C}R$ isoforms (TM1 through TM7). *B*, Diagram of the exon/intron structure of the rat $H_3R$ gene on chromosome 3 (Genbank accession number NM_053506.1 (GI:16758263)) and the resulting amino acid (aa) sequences found in $rH_{3A\text{-}C}$ receptors and $rH_{3D\text{-}E}$ isoforms generated by retention/deletion of the pseudo-introns. The exon/intron junctions within the $rH_3R$ gene are indicated in bold (**GT** and **AG**), whereas the codon that corresponds to the cysteine (C) found in the $rH_{3D\text{-}F}$ isoforms (formed by TG and T) is underlined. For simplicity, only part of the exon/intron structure of the rat $H_{3R}$ gene and of the $rH_3R$ gene sequence is shown (as indicated by //). See (Morisset et al., 2001) for an overview of the exon/intron structure of the $rH_3R$ gene corresponding to the two presumably non-functional $H_3R$ isoforms, $H_{3(nf1)}$ and $H_{3(nf2)}$, and the four previously described functional shorter isoforms, $rH_{3B}$ ($rH_{3(413)}$), $rH_{3(410)}$, and $rH_{3C}$ ($rH_{3(397)}$).

Figure 2. Topology of the $rH_3R$ isoforms. Prediction of the topology of the $rH_{3A}R$ (*A*) *versus* the $rH_{3D}R$ (*B*), as predicted by the TMHMM Server at the Center for Biological Sequence Analysis, Technical University of Denmark, DTU (http://www.cbs.dtu.dk/services/TMHMM/). Indicated

Molecular Pharmacology Fast Forward. Published on January 13, 2006 as DOI: 10.1124/mol.105.019299
This article has not been copyedited and formatted. The final version may differ from this version.



by the solid line are the probabilities for localisation on the extracellular side (outside); the pobabilities of localisation on the intracellular side (Inside) are indicated by the dotted lines. The probability for transmembrane (TM) domains are indicated by the filled areas. From these two plots it can be deducted that seven TM domains are predicted for the $rH_{3A}R$ while for the $rH_{3D}R$ only six TM domains are predicted, as indicated above the graphs. *C*, Graphical representation of the topology of the $rH_{3A}$, $rH_{3B}$, and $rH_{3C}$ receptors, *versus* the $rH_{3D}$, $rH_{3E}$, and $rH_{3F}$ isoforms (*D*). In contrast to the $rH_{3A}$, $rH_{3B}$, and $rH_{3C}$ receptors, the $rH_{3D}$, $rH_{3E}$, and $rH_{3F}$ isoforms are predicted to possess an extracellular C-terminal domain. Also indicated in *C* and *D* are the variations in the third intracellular loop between the isoforms. *E* and *F*, Immunological detection of N-terminally HA-tagged $rH_{3A}Rs$ (HA-$rH_{3A}$) and the N-terminally HA-tagged $rH_{3D}$ isoform (HA-$rH_{3D}$) on transfected COS-7 cells. E, Detection of HA-$rH_{3A}Rs$ and the HA-$rH_{3D}$ isoform in intact cells *versus* cells that have been permeabilised using 0.5% NP-40 in an ELISA assay. *F*, Immunocytochemical detection of HA-tagged $rH_3R$ isoforms using a rhodamine conjugated antibody directed against the HA-tag. Detection of HA-$rH_{3A}Rs$ on intact COS-7 cells (upper panel, left) and in permeabilised cells (upper panel, right). Detection of the HA-$rH_{3D}$ isoform on intact cells (bottom panel, left) and in permeabilised cells (bottom panel, right).

Figure 3. Functional analysis of the $rH_{3A}R$ and the $rH_{3D}$ isoform upon transient transfection of their corresponding cDNAs in COS-7 cells. *A*, Transfection of cells with $rH_{3A}R$ coding cDNA ($pcDEF_3rH_{3A}R$; 5 $\mu g/10^6$ cells) resulted in the expression of $^{125}$IPP binding sites, whereas no specific $^{125}$IPP binding was detected to membrane fractions of cells transfected with an equal amount of cDNA coding for either the $rH_{3D}$, $rH_{3E}$, or $rH_{3F}$ isoform. *B*, Dose dependent modulation of 10 $\mu$M forskolin induced responses by histamine, immepip, and R($\alpha$)-

Molecular Pharmacology Fast Forward. Published on January 13, 2006 as DOI: 10.1124/mol.105.019299
This article has not been copyedited and formatted. The final version may differ from this version.



methylhistamine using COS-7 cells co-transfected with 5 μg/$10^6$ cells of both pcDEF$_3$rH$_{3A}$R and a CREB-responsive firefly-luciferase reporter gene (pTLNC121CRE). *C*, Modulation of forskolin (10 μM) induced responses by 10 μM of histamine, R(α)-methylhistamine (RαMH), and thioperamide using cells transfected with both pcDEF$_3$rH$_{3A}$R and pTLNC121CRE. The forskolin induced responses are set to 100% as indicated by "control". *D*, Effects of 10 μM R(α)-methylhistamine on forskolin (10 μM) induced responses using cells co-transfected with either pcDEF$_3$rH$_{3A}$R, pcDEF$_3$rH$_{3D}$, pcDEF$_3$rH$_{3E}$, or pcDEF$_3$rH$_{3F}$, and pTLN121CRE. The forskolin induced responses are set to 100% as indicated by the dashed line.

Figure 4. Immunological detection of N-terminally HA-tagged rH$_{3A}$Rs (HA-rH$_{3A}$) on COS-7 cells co-transfected with cDNA coding for HA-rH$_{3A}$ receptors and the N-terminally HA-tagged rH$_{3D}$ isoform (HA-rH$_{3D}$). *A*, Effects of the co-transfection of pcDEF$_3$rH$_{3D}$ on the detection of HA-rH$_{3A}$Rs on intact cells using an ELISA assay. *B*, Immunocytochemical detection of HA-rH$_{3A}$Rs using a rhodamine conjugated antibody directed against the HA-tag. Detection of HA-rH$_{3A}$Rs on intact COS-7 cells (upper panel, left) and in permeabilised cells (upper panel, right), and effects of co-transfection cells with both pcDEF$_3$-HA-rH$_{3A}$ and pcDEF$_3$rH$_{3D}$ on the detection of the HA-rH$_{3A}$Rs on intact cells (bottom panel, left) and in permeabilised cells (bottom panel, right). Control slides of cells transfected with N-terminally HA-epitope tagged H$_3$ isoforms that did not receive the primary antibody or of untransfected cells showed no appreciable staining.

Figure 5. Effects of co-transfection of cDNA coding for rH$_3$R isoforms on the expression of $^{125}$IPP binding sites. Evaluation of the effects of co-transfection of either 0.25 μg/$10^6$ cells of pcDEF$_3$rH$_{3A}$R (*A*, *B*, *C*, *D*, and *E*), pcDEF$_3$rH$_{3B}$R (*F*), or pcDEF$_3$rH$_{3C}$R (*G*) together with varying

Molecular Pharmacology Fast Forward. Published on January 13, 2006 as DOI: 10.1124/mol.105.019299
This article has not been copyedited and formatted. The final version may differ from this version.



amounts (0 - 2.5 μg/$10^6$ cells) of either pcDEF$_3$rH$_{3D}$ (*A*), pcDEF$_3$rH$_{3E}$ (*B*, and *F*), pcDEF$_3$rH$_{3F}$ (*C*, and *G*), pcDEF$_3$hH$_1$ (*D*), pcDEF$_3$rH$_2$R (*E*), or pcDEF$_3$ORF74 (*E*) on the relative number of expressed $^{125}$IPP binding sites. *H*, Evaluation of the effects of co-transfection of pcDEF$_3$rH$_{3A}$R (0.25 μg/$10^6$ cells) together with 2.5 μg/$10^6$ cells of either pcDEF$_3$rH$_{3D}$ (○) or pcDEF$_3$hH$_1$ (●) on the ability of IPP to displace $^{125}$IPP bound to expressed $^{125}$IPP binding sites (homologous displacement).

Also shown in *E* are the effects of the transfection of 2.5 μg/$10^6$ cells of either pcDEF$_3$rH$_{3A}$R, pcDEF$_3$rH$_2$R, pcDEF$_3$ORF74, or pcDEF$_3$rH$_{3D}$ alone on the expression of $^{125}$IPP binding sites. The proper expression in COS-7 cells of the hH$_1$R, the rH$_2$R, and ORF74 was confirmed using [$^3$H]mepyramine, $^{125}$I-APT, and $^{125}$I-CXCL8 binding assays, respectively (data not shown). In each condition the total amount of cDNA has been kept constant using pcDEF$_3$.

Figure 6. Effects of co-transfection of the rH$_{3D}$ isoform on the function of the rH$_{3A}$R. *A*, Dose dependent modulation of 10 μM forskolin induced responses by histamine, immepip, and R(α)-methylhistamine using PTX treated (100ng/ml) COS-7 cells co-transfected with 5 μg/$10^6$ cells of both pcDEF$_3$rH$_{3A}$R-G$\alpha_{o1}$C$^{351}$I and a CREB-responsive firefly-luciferase reporter gene (pTLNC121CRE). *B*, Evaluation of the effects of co-transfection of 0.25 μg/$10^6$ cells of pcDEF$_3$rH$_{3A}$R-G$\alpha_{o1}$C$^{351}$I together with varying amounts of pcDEF$_3$rH$_{3D}$ (0 - 2.5 μg/$10^6$ cells) on the relative number of expressed $^{125}$IPP binding sites. *C*, Effects of the co-transfection of 0.25 μg/$10^6$ cells pcDEF$_3$rH$_{3A}$R and 2.5 μg/$10^6$ cells pcDEF$_3$rH$_{3D}$ on [$^{35}$S]GTPγS binding to the PTX-insensitive mutant G$\alpha_{o1}$C$^{351}$I protein fused to the C-terminal domain of the rH$_{3A}$R (rH$_{3A}$R-G$\alpha_{o1}$C$^{351}$I fusion protein). Shown are the effects of co-transfection of pcDEF$_3$rH$_{3D}$ on the H$_3$R agonist immepip (1 μM)-induced [$^{35}$S]GTPγS binding to the rH$_{3A}$R-G$\alpha_{o1}$C$^{351}$I fusion protein in

Molecular Pharmacology Fast Forward. Published on January 13, 2006 as DOI: 10.1124/mol.105.019299
This article has not been copyedited and formatted. The final version may differ from this version.



PTX-treated cells (100 ng/ml), and the effects of the inverse $H_3R$ agonist thioperamide (1 μM) on the 1 μM immepip-induced [$^{35}$S]GTPγS binding. Shown are the averages of three independent experiments.

Figure 7. Detection of oligomerisation of heterologous and native $rH_{3A}Rs$. *A*, Biochemical evidence for $rH_{3A}R$ oligomers. Membranes derived from either cells heterologously expressing $rH_{3A}Rs$ or from native rat forebrain membranes were analysed by immunoblotting (*lanes 1-3* and *4*, respectively) as described in the materials and methods section. In addition, samples of membranes expressing $rH_{3A}Rs$ were subjected to chemical crosslinking with either 0.12mM or 0.25mM BS3 (*lanes 2* and *3*, respectively) prior to immunoblotting. Lanes 1-3 were subsequently probed with rabbit anti-$H_{3C}$ 268-277Cys antibody (0.2 μg/ml), and lane 4 was probed with rabbit anti-$H_3$ 349-358 antibody (1.5 μg/ml). The immunoblot is representative of at least three separate experiments. The molecular weight ($M_r$) standards are displayed on the left and are indicated in kDa. *B*, Detection of dimeric $rH_{3A}Rs$ by *time-resolved* FRET (*tr*-FRET). Upon measuring fluorescence emission at 665 nm, after excitation at 337 nm, tr-FRET signals are seen using live cells expressing HA-$rH_{3A}Rs$, due to the resonance energy transfer of specific HA-$rH_{3A}Rs$ bound to anti-HA-$Eu^{3+}$ antibody to the specific HA-$rH_{3A}Rs$ bound to anti-HA-allophycocyanin antibody. *tr*-FRET signals were seen only using membranes of HA-$rH_{3A}R$ expressing cells that were co-incubated with both the anti-HA-$Eu^{3+}$ ($Eu^{3+}$) antibody and the anti-HA-allophycocyanin (XL665) antibody ($Eu^{3+}$ + XL665). Mixing of two populations of cells expressing HA-$rH_{3A}Rs$ independently incubated with either anti-HA-$Eu^{3+}$ or anti-HA-allophycocyanin antibodies resulted in a reduced *tr*-FRET signal. Data are plotted as as the *tr*-FRET that is observed using HA-$rH_{3A}R$ expressing cells that have been incubated with both anti-HA-$Eu^{3+}$ and anti-HA-

Molecular Pharmacology Fast Forward. Published on January 13, 2006 as DOI: 10.1124/mol.105.019299
This article has not been copyedited and formatted. The final version may differ from this version.



allophycocyanin antibodies *versus* the *tr*-FRET that is observed using a mix of two populations of HA-r$H_{3A}$R expressing cells that proir to mixing were independently incubated with with either of the two antibodies.

Figure 8. Detection of r$H_3$ isoform mRNA in rat brain. *A*, Diagrammatic representation of mRNA sequences recognized by probes $H_{3AD}$ and $H_{3DEF}$. *B*, mRNA levels of isoforms detected with probe $H_{3AD}$. *C*, Images of representative sections from control and 48h post-PTZ injection animals. *D*, Expression mRNA levels of isoforms detected with probe $H_{3DEF}$. *E*, Images of representative sections from control and 24h post-injection. Data are presented as IOD ± SEM; levels of significance are as follows: *$p < 0.05$; **$p < 0.01$; ***$p < 0.001$. Abbreviations: ctx II-VIb, cortex layers II to VIb; CPu, caudate putamen; Pir, piriform cortex; CA1, CA1 region of the hippocampus; CA3, CA3 region of the hippocampus.

Molecular Pharmacology Fast Forward. Published on January 13, 2006 as DOI: 10.1124/mol.105.019299
This article has not been copyedited and formatted. The final version may differ from this version.

**A**

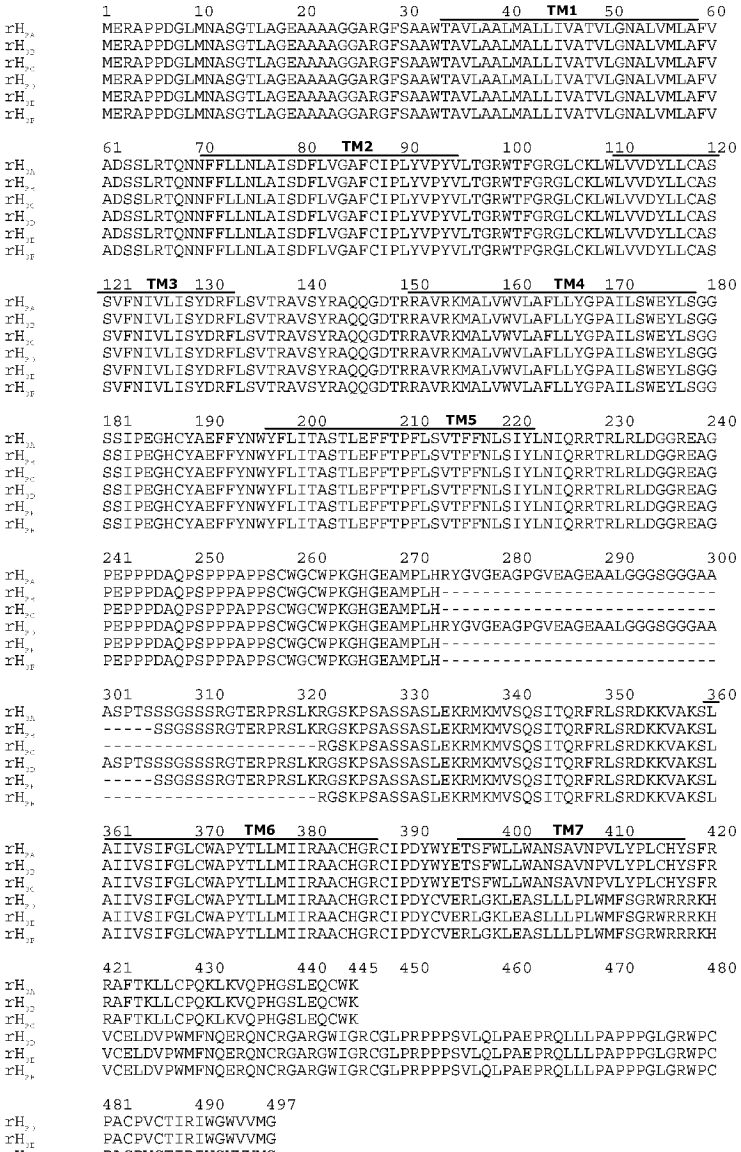


**B**

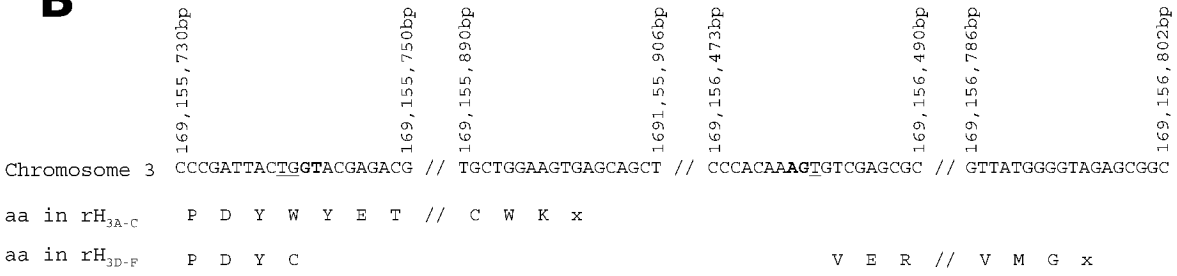


**Figure 1**

Molecular Pharmacology Fast Forward. Published on January 13, 2006 as DOI: 10.1124/mol.105.019299
This article has not been copyedited and formatted. The final version may differ from this version.

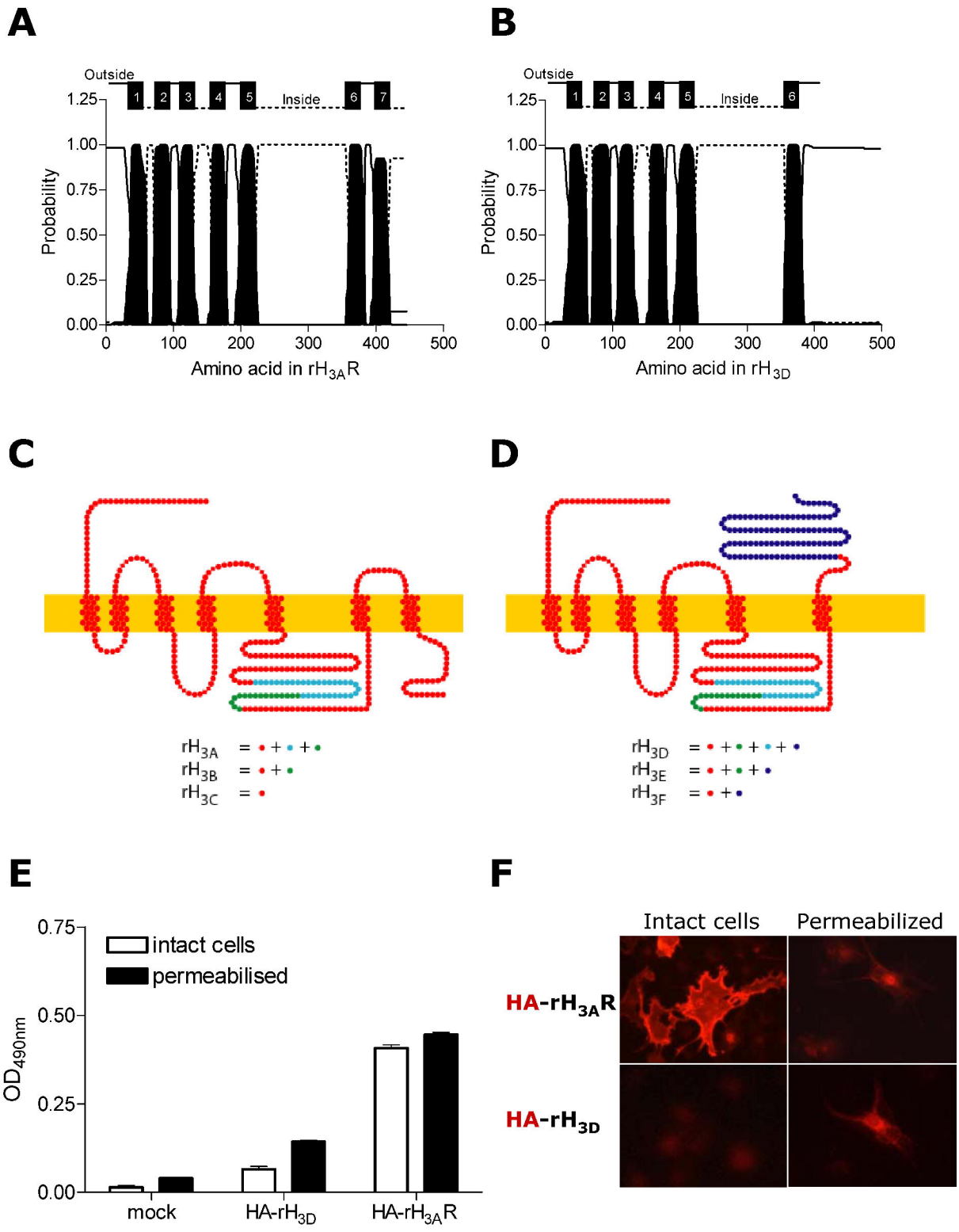


**Figure 2**

Molecular Pharmacology Fast Forward. Published on January 13, 2006 as DOI: 10.1124/mol.105.019299
This article has not been copyedited and formatted. The final version may differ from this version.

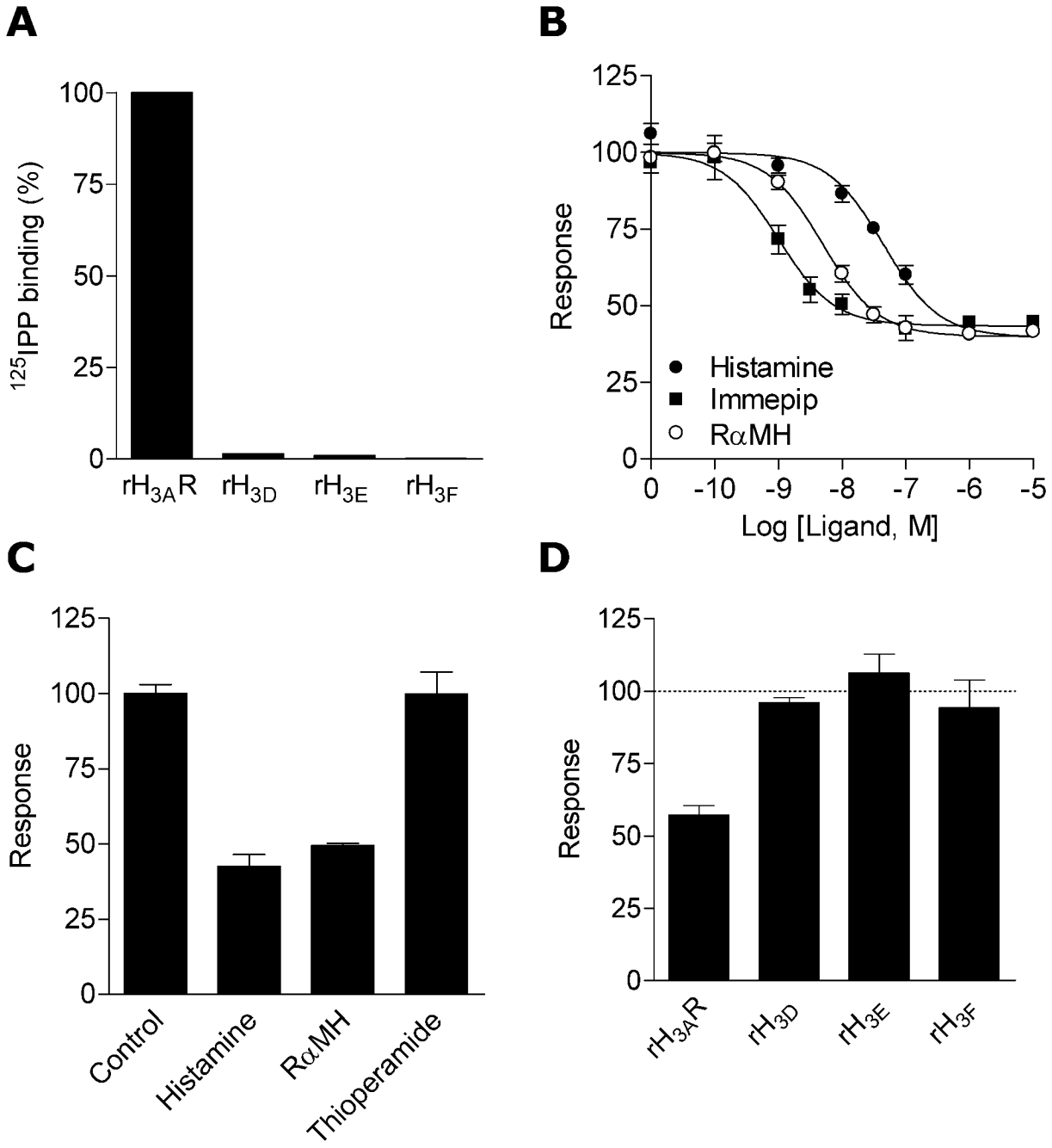


**Figure 3**

Molecular Pharmacology Fast Forward. Published on January 13, 2006 as DOI: 10.1124/mol.105.019299
This article has not been copyedited and formatted. The final version may differ from this version.

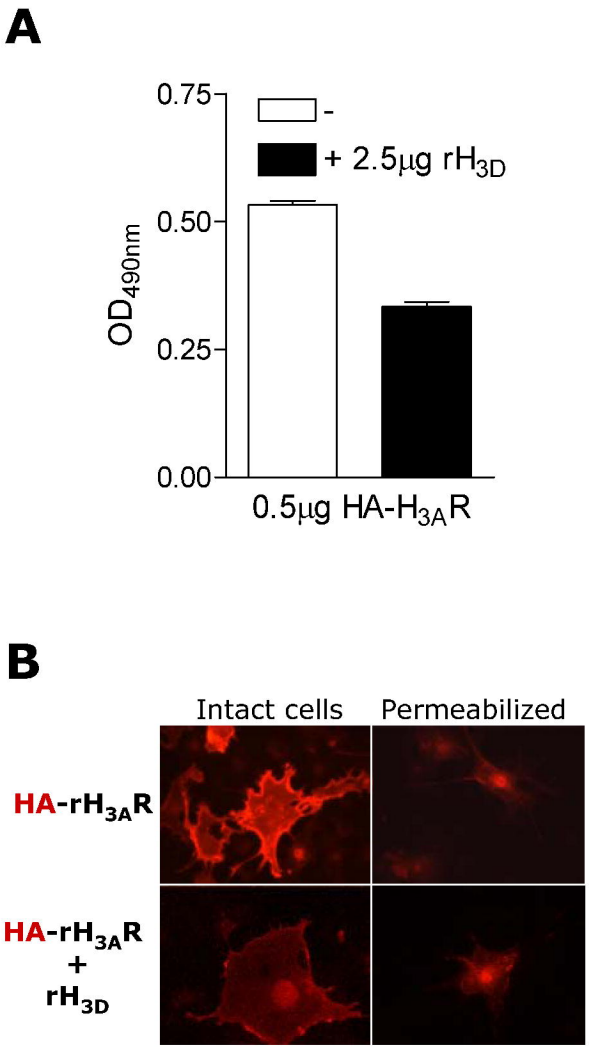


**Figure 4**

Molecular Pharmacology Fast Forward. Published on January 13, 2006 as DOI: 10.1124/mol.105.019299
This article has not been copyedited and formatted. The final version may differ from this version.

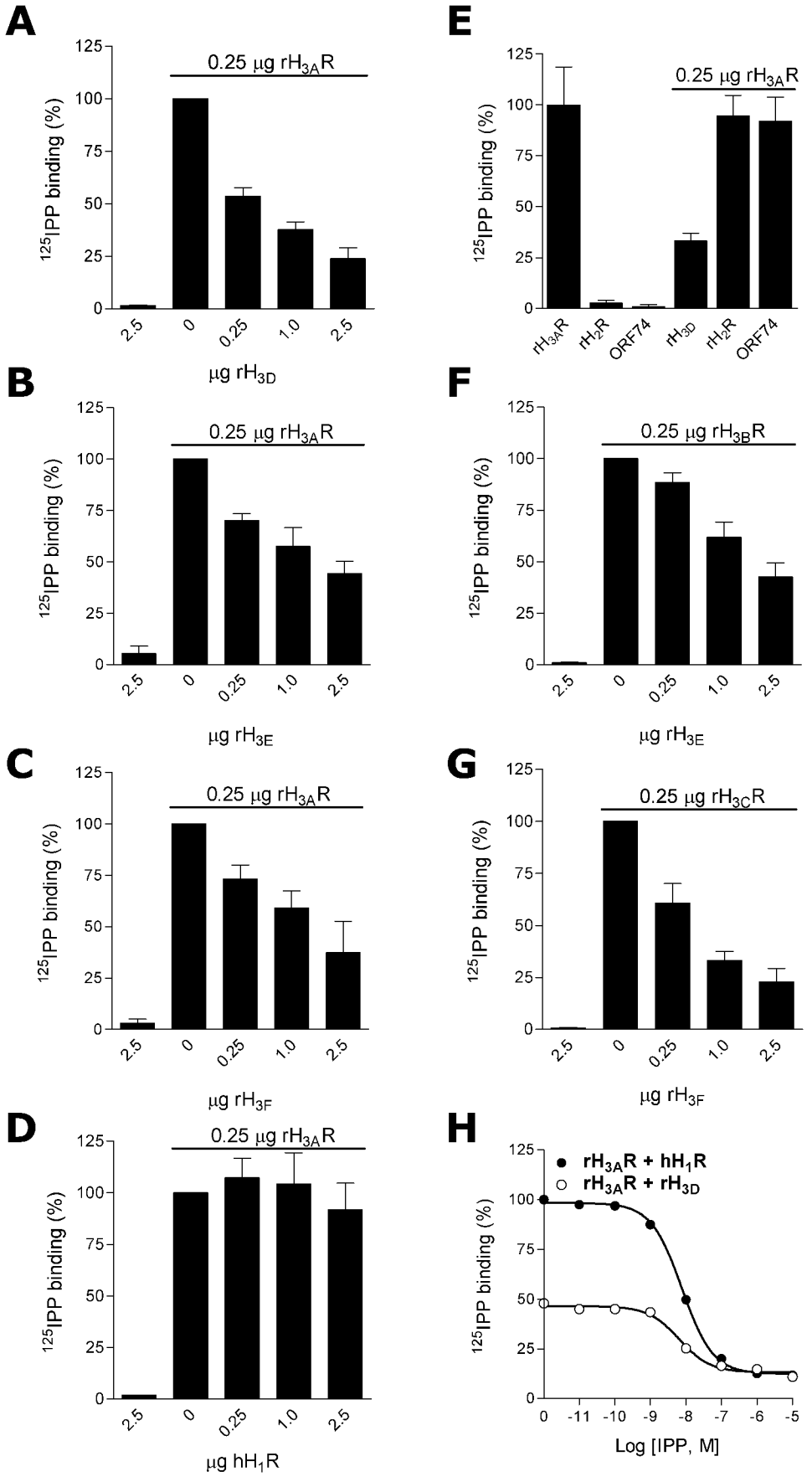


**Figure 5**

Molecular Pharmacology Fast Forward. Published on January 13, 2006 as DOI: 10.1124/mol.105.019299
This article has not been copyedited and formatted. The final version may differ from this version.

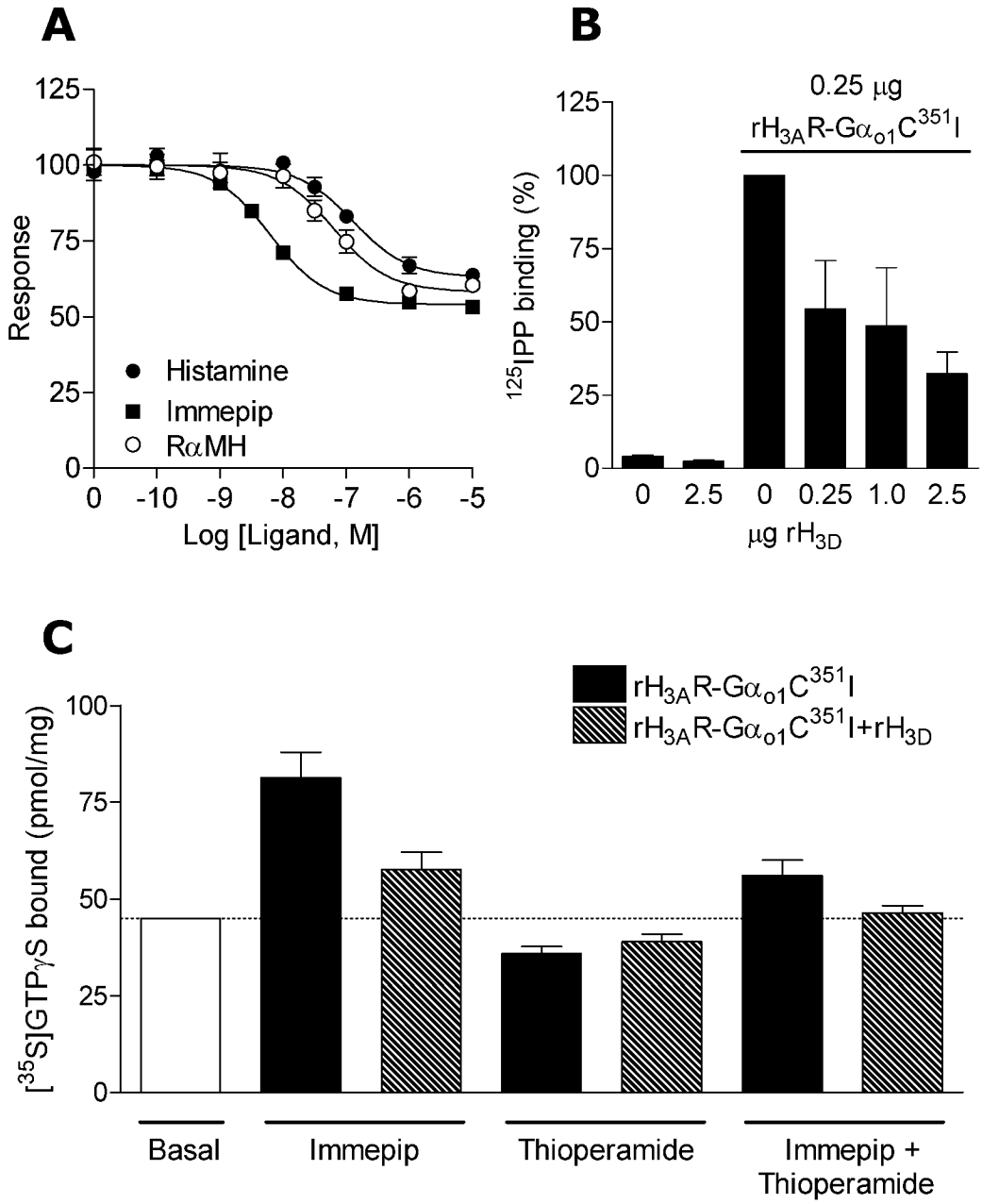


**Figure 6**

Molecular Pharmacology Fast Forward. Published on January 13, 2006 as DOI: 10.1124/mol.105.019299
This article has not been copyedited and formatted. The final version may differ from this version.

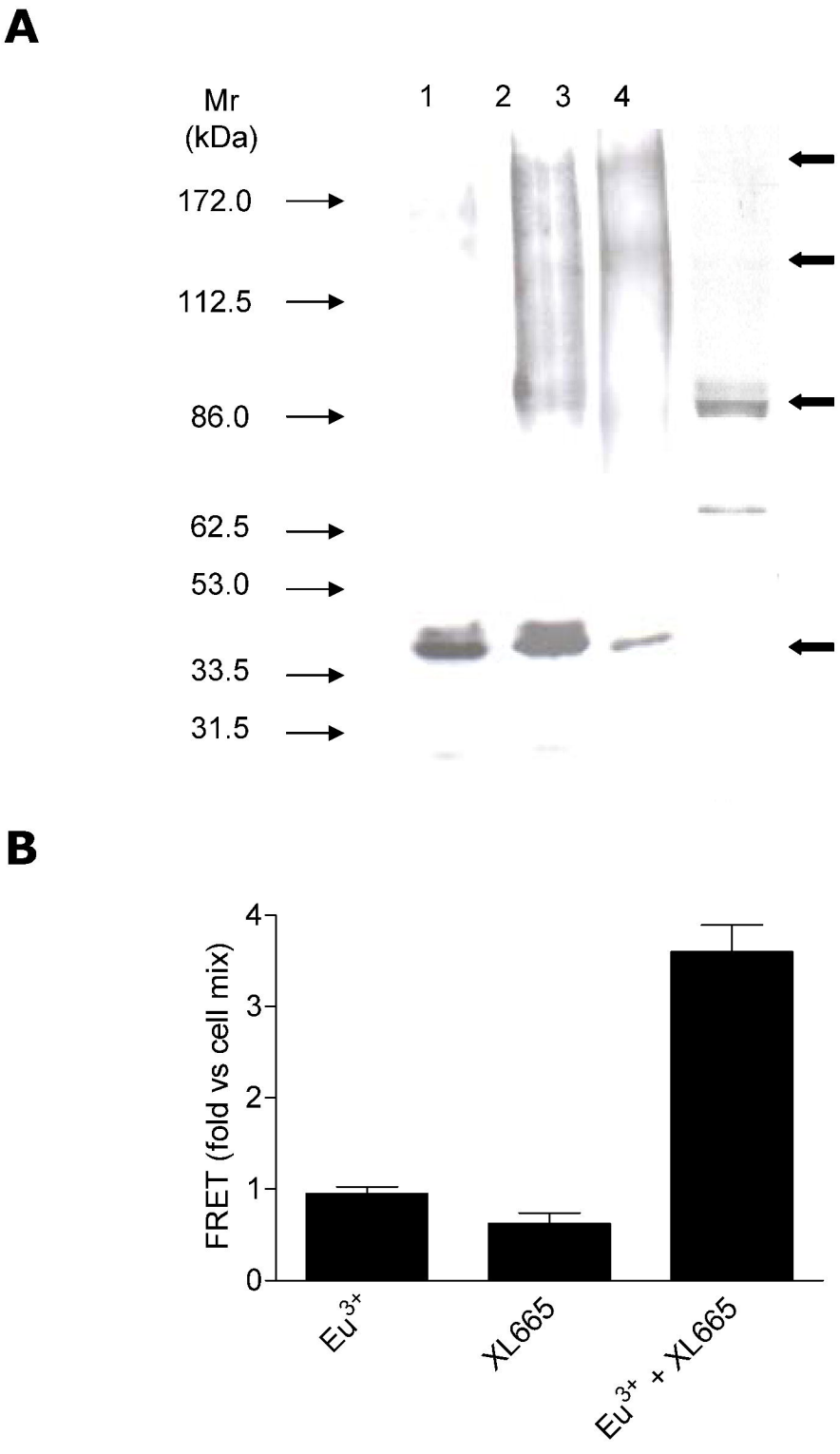


**Figure 7**

Molecular Pharmacology Fast Forward. Published on January 13, 2006 as DOI: 10.1124/mol.105.019299
This article has not been copyedited and formatted. The final version may differ from this version.

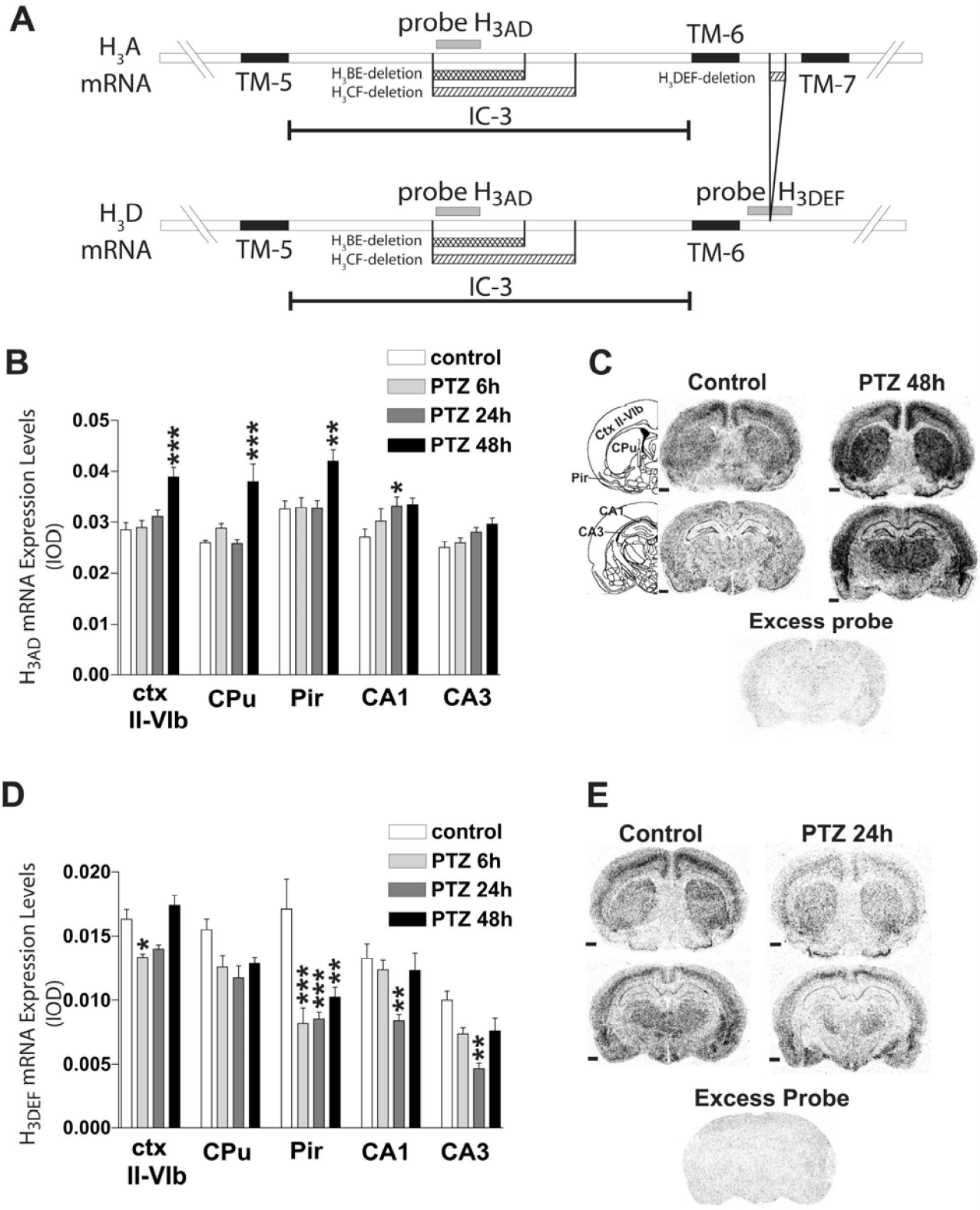


**Figure 8**